Electron collisions with highly polar molecules: Comparison of model, static, and static-exchange calculations for alkali-metal halides

L. A. Collins* and D. W. Norcross†

Joint Institute for Laboratory Astrophysics, National Bureau of Standards and University of Colorado, Boulder, Colorado 80309

(Received 20 March 1978)

Calculations of cross sections for (vibrationally and electronically) elastic collisions of electrons with several alkali-metal halides were performed for energies in the range of 0.13 to 20.0 eV. The applicability of the adiabatic (fixed-nuclei) approximation for strongly polar systems is investigated by model calculations on CsF, KI, and LiF. We demonstrate that integrated, momentum transfer, and differential cross sections for polar systems can be reliably generated entirely within the body-frame, adiabatic approximation. We also suggest resolutions of several discrepancies between the results of earlier calculations and between these results and measurements. Close-coupling calculations, based on the adiabatic approximation and an alternative form of the frame transformation, were performed for electron-LiF collisions using the full static and static model-exchange surface. Reasonable agreement was found with measured differential cross sections at 5.44 and 20.0 eV. Shape resonances in the Σ and Π body-frame symmetries, centered near 1.8 and 1.5 eV, respectively, were observed. Similar features appeared in static-exchange calculation for NaF and NaCl. We also compare the results of the static and static-exchange calculations with the results of calculations using simpler model potentials and other approaches to the collision problem.

I. INTRODUCTION

The scattering of electrons by molecules with permanent dipole moments has been intrinsically interesting ever since Massey observed[1] in 1932 that "... the collision of electrons with a top possessing such a dipole moment may be treated by Born's method (italics ours) *whatever the velocity of the electrons may be.*" The assumption that the interaction is dominated, if not completely determined, by the long-range dipole potential, leads to extremely simple cross-section formulas that depend only on the electron kinetic energy, and the molecular dipole moment and moment of inertia (i.e., rotational spacing). These formulas provide not only useful estimates of cross sections in some cases but also a framework for more-elaborate calculations and a benchmark against which the results of such calculations and of measurements can be compared.

We will find it useful in what follows to present and briefly discuss these formulas at the outset. For a molecule initially in rotor state j with dipole moment D in a.u. (=2.5418 D), and an incident electron with kinetic energy k^2 in $\mathcal{R}_\infty$ (=13.606 eV), the differential,[2] momentum transfer,[2] and integrated[3] cross sections in the first Born approximation (FBA) can be written (for a rotating dipole)

$$\frac{d\sigma}{d\Omega}(j\to j'|\theta)=\tfrac{4}{3}D^2\frac{j_>}{2j+1}\frac{k'}{k}\times\frac{1}{(k^2+k'^2-2kk'\cos\theta)}, \tag{1.1}$$

$$\sigma_M(j\to j')=\frac{8\pi}{3k^2}D^2\frac{j_>}{2j+1}\left(1-\frac{(k-k')^2}{2kk'}\ln\frac{k+k'}{|k-k'|}\right), \tag{1.2}$$

and

$$\sigma_I(j\to j')=\frac{8\pi}{3k^2}D^2\frac{j_>}{2j+1}\ln\frac{k+k'}{|k-k'|}, \tag{1.3}$$

where $j'=j\pm1$, k'^2 is the kinetic energy of the outgoing electron, and $j_>$ is the larger of j and j'. All cross sections are in units of a_0^2 (=0.28 003 $\times10^{-20}$ m^2). Atomic units are used throughout this paper, unless otherwise noted.

We note immediately that the FBA predicts exceedingly large cross sections for molecules with large moments of inertia and/or large dipole moments. In the limit of the moment of inertia I tending to infinity, k' goes to k, and hence (1.1) diverges in the forward direction and (1.3) is infinite. The total (summed over j') differential and momentum-transfer cross sections reduce in this limit to

$$\frac{d\sigma}{d\Omega}(\theta)=\frac{2}{3k^2}D^2\frac{1}{1-\cos\theta} \tag{1.4}$$

and

$$\sigma_M=(8\pi/3k^2)D^2, \tag{1.5}$$

which are independent of j. These results were first obtained in the adiabatic approximation,[4] i.e., by assuming that the duration of the collision is short compared with the rotational period and considering *elastic* scattering by a *fixed* dipole.

Given the magnitude of the cross sections predicted by the FBA, and the fact that polar mo-

lecules (e.g., H_2O, CO, CN, and KOH) are known to exist in a wide variety of laboratory, atmospheric, and astrophysical plasmas, interest in electron scattering by this class of molecules obviously goes beyond being purely academic. Successful modeling of the processes occurring in these plasmas requires elucidation of the conditions for which the simple formulas (1.1)–(1.3), or (1.4) and (1.5), are quantitatively, as well as qualitatively, correct, or data of considerably greater accuracy.

An extensive literature[5] has accumulated since Massey's original work, in the effort to test, and improve upon, the FBA and to obtain accurate data for a wide variety of polar molecules. Most of this work involved molecules with relatively small dipole moments ($D \lesssim 1.5$ a.u.), and for quite low-energy electrons ($\ll 1$ eV). The only experimental data available until quite recently were obtained from thermal-energy-swarm experiments, which measure electron diffusion and drift velocities in gases of polar molecules (cf. Ref. 2).

The state of knowledge as of about 1972 with regard to the general aspects of this problem has been succinctly summarized by Garrett[6]: "It has been well established that thermal-energy momentum transfer and elastic cross sections for electrons on polar molecules cannot be determined to any reasonable degree of approximation by considering only the dipole contribution to the electron-molecule interaction potential. However (integrated) rotational-excitation cross sections show a very strong correlation with the square of the dipole moment of the target system and are reasonably well represented by the result obtained from the Born approximation." While Garrett's systematic model studies[7] demonstrated the importance of short-range interactions and induced polarization, at least for thermal-energy electrons and molecules with $D \lesssim 1.5$ a.u., the absence of either high-precision single-collision measurements or detailed calculations for any molecule with a significant dipole moment made it impossible to quantify the exact "degree of approximation" involved in simple theoretical models.

Much more work was clearly required, and it has received great stimulus recently from the molecular-beam-recoil measurements of Stern and co-workers.[8-11] These were[8] "the first absolute, single-collision measurements on a molecule of significant polarity, and therefore a first test for features of the theory." These measurements were made for electron energies $\gtrsim 0.5$ and $\lesssim 15$ eV, and for molecules (CsF, CsCl, and KI) with dipole moments ranging from 3.10 to 4.26 a.u.

The results were surprising, particularly for low-energy electrons (~1 eV). The differential cross sections were much more strongly peaked at very small angles, and very much smaller elsewhere, than the FBA prediction; and the total integrated (momentum-transfer) cross section ranged from a factor of 2–3 (10–20) times smaller than the FBA prediction at the lowest energies. Pronounced minima in the differential cross sections were found at 60°–90° and at 180°. More recent relative crossed-beam measurements[12] for KI yielded results for the shape of the differential cross section which did not show the pronounced minima previously observed, except at the much higher energy of 60 eV. Results qualitatively similar to the latter have been obtained very recently for LiF.[13]

There have been a great number and variety of calculations made in recent years in the effort to understand the results of these measurements. In order to put our own work in sharper perspective we will discuss the results of these calculations in Sec. II. It suffices here to say that all of these calculations, no matter how sophisticated the treatment of the scattering equations, have employed quite simple models of the interaction potential. While there can be no doubt that these calculations have provided an extremely useful qualitative understanding of the scattering process, particularly the limited validity of the FBA, they also confirm the observation of Garrett quoted above, as we shall see.

We have, therefore, undertaken a detailed study of electron scattering by the typical highly polar molecule LiF using the close-coupling formalism and a much more accurate representation of the interaction potential (including static, exchange, and polarization effects) than in any previous calculations for a highly polar molecule.[14] This molecule was chosen, rather than one of those for which measurements had already been made, because a Hartree-Fock wave function is available, and because it is the simplest alkali-metal halide to treat computationally. We also report the results of preliminary calculations in the same approximation for LiCl, NaF, and NaCl.

In order to investigate several qualitative aspects of the scattering process, and the utility of much simpler representations of the interaction potential and treatments of the scattering formalism, we have performed close-coupling calculations for LiF, CsF, and KI using model potentials similar to those used in other work. For LiF, we have also employed restricted approximations to the complete static (no exchange) interaction potential. Finally, we have investigated two

unitarized Born approximations,[15] which are simple variations on the FBA.

The rest of this paper is organized as follows. In Sec. II we briefly discuss the application and validity of a commonly used approximation in electron-molecule scattering, the adiabatic approximation, and summarize some of the issues raised by recent theoretical and experimental results. We present in Sec. III the basic scattering formalism used in the present work. This includes discussion of both the space-fixed (laboratory) and body-fixed (adiabatic) reference frames, the collisional approximations, and the interaction potentials employed. In Sec. IV we describe in detail the techniques used to solve the scattering equations in the close-coupling approximation, the generation of cross sections, and the convergence (accuracy) criteria imposed. The results are presented and discussed in Sec. V, and our conclusions summarized in Sec. VI.

II. BACKGROUND

It would be inappropriate to attempt here a detailed review of all the models proposed, and calculations made, for electron scattering by highly polar molecules in recent years. It will be useful, however, to comment briefly on the conclusions which have been drawn from this work, and to summarize the major insights that have been gained. This discussion will also highlight some of the ambiguities which may attend an intercomparison of earlier results and provide the motivation for some of the specific comparisons of the results of other work, both theoretical and experimental, with our own in Sec. V.

One of the major difficulties attending any attempt to compare the results of calculations with the measurements cited above is the fact that the latter were carried out with molecular beams at temperatures on the order of 1000 °K. One then has a distribution of molecular rotational states populated statistically about some most probable value which is quite high, typically $\bar{j} = 40$–80 for the molecules studied by Stern and co-workers.[8-11]

Faced with this fact the theorist has three options: (i) calculations for molecules with initial values of j typical of the experimental conditions, which become exceedingly difficult the more sophisticated the scattering formalism and interaction potential adopted; (ii) use of the adiabatic approximation (mentioned in Sec. I in the context of the FBA and discussed in more detail below), in which case the cross sections obtained, when summed over all final rotational states assumed degenerate in energy, are independent of j; or (iii) calculations for a molecule with j small or zero, in which case direct comparison with experimental measurements cannot be made without the invocation of the same assumptions that underlie the adiabatic approximation. Because of the critical importance of this approximation to many of the calculations made to date, and to our own work, we will first discuss it in some detail.

A. Adiabatic approximation

This approximation has been used with considerable success in calculations of electron scattering by homonuclear (nondipolar) molecules. It is not obvious, however, that the approximation can be applied in calculations of electron scattering by polar molecules, in view of the long-range nature of the dipole potential. In fact, as is well known, forward-scattering and integrated cross sections diverge if this approximation is consistently adopted. This divergence has already been noted in Sec. I for the special case of the FBA, and may be partially responsible for skepticism about the validity of this approximation for differential cross sections for scattering out of the forward direction and for momentum-transfer cross sections as well, in spite of evidence to the contrary for the special case of the FBA. Much of the recent theoretical evidence seems to support this skepticism.

We believe, however, that this evidence is misleading and that the adiabatic approximation can, when carefully applied, be extremely useful at little or no sacrifice in accuracy in calculations for polar molecules. Essentially classical arguments in support of this hypothesis are reviewed below. The implications for quantum-mechanical calculations will be discussed in Sec. III C.

In order to distinguish the results of calculations which involve this approximation in one way or another, we first define the "complete" representation as that in which the rotational Hamiltonian of the target molecule is explicitly included in the wave equation for the scattering system.

The fundamental criterion[16] for the validity of the adiabatic approximation is that

$$|k - k'|R_e \ll 1 , \tag{2.1}$$

where R_e is some effective radius for the interaction region. Classically stated, this condition requires that for a projectile with velocity v the duration of the collision $R_e a_0/v$ be short compared with the period ω^{-1} of target motion. For electron-molecule scattering this condition is often used to justify neglect of the rotational Hamiltonian

of the target (we will ignore here vibrational and electronic degrees of freedom), from which it follows that the wave function for the scattered electron may be obtained with the positions of the molecular nuclei held momentarily fixed in space. This can be viewed as a sudden approximation in the motion of the electron.

With this approximation scattering amplitudes for rotationally elastic and inelastic transitions can be obtained by a simple rotational transformation to the coordinate frame in which the molecule rotates. We will refer to this henceforth as the adiabatically rotating molecule (ARM) representation.

Cross sections for elastic scattering by an ensemble of molecules assumed to be motionless and randomly oriented in space may also be obtained by averaging the scattering amplitude for the fixed molecule over all orientations relative to the incident electron direction. This will be referred to henceforth as the fixed-nuclei (FN) representation. (The phrase "fixed nuclei" is also occasionally used to designate what we refer to as the ARM representation.) It has been shown[17] that the total (summed over all final rotor states) differential cross section in the ARM representation is independent of the initial rotor state and identical to the elastic differential cross section in the FN representation. This result similarly applies to the total integrated and momentum-transfer cross sections as well.

Limitations on the validity of the adiabatic approximation will clearly apply equally to calculations carried out in the ARM and FN representations. This is conventionally[4] assessed by evaluating R_e from the classical distance of closest approach,

$$k^2 = D/R_e^2 . \tag{2.2}$$

With (2.2) the condition (2.1) for the validity of the adiabatic approximation becomes

$$\delta = \frac{D^{1/2}|k-k'|}{k} \simeq \frac{D^{1/2}|k^2-k'^2|}{2k^2} \ll 1 , \tag{2.3}$$

which is well satisfied for most electron-molecule collision systems of interest.

The divergence of the forward-scattering and integrated cross sections in the FN representation is, on the other hand, an essential property of the dipole potential. It is not just a special consequence of the FBA for the point-dipole potential, nor could it be avoided by any more sophisticated treatment of the scattering problem for a polar molecule in the FN representation.[18] This follows from the facts that divergence in the FBA cross sections is owing to a logarithmic divergence in the partial-wave series for large l (the angular momentum of the scattered electron), and that the interaction is, in the limit of large l, accurately treated using the FBA for the point-dipole potential.

The resolution of the apparent contradiction between the conclusion based on (2.3) and the complete breakdown of the adiabatic approximation for forward scattering follows from the observation that (2.2) is inappropriate for small-angle (large-impact-parameter) scattering. For impact parameters $R_e \gtrsim 4D/k$, or equivalently for scattering angles

$$\theta \lesssim 1/8D = \theta_1 , \tag{2.4}$$

it is necessary to adopt instead a quantum mechanical description.[19] The FBA formulas (1.1)–(1.3) for the point-dipole potential in the complete representation are adequate for this limited purpose. Thus no real contradiction exists. The adiabatic approximation may be invalid for transitions with $|\Delta j| = 1$ at small scattering angles, but (2.3) remains a valid criterion for assessing its validity for $\theta \gtrsim \theta_1$.

Let us consider, then, the angular region $\theta \lesssim \theta_1$ in a situation in which $\delta \ll 1$. In this limit we can approximate (1.1)–(1.3) by

$$\frac{d\sigma}{d\Omega}(j \to j'|\theta) \simeq \frac{3}{2k^2} D^2 \frac{j_>}{2j+1} \frac{1}{1-\cos\theta+2\Delta} , \tag{2.5}$$

$$\sigma_M(j \to j') \simeq \frac{8\pi}{3k^2} D^2 \frac{j_>}{2j+1} (1 + \Delta \ln\Delta) , \tag{2.6}$$

and

$$\sigma_I(j \to j') \simeq \frac{4\pi}{3k^2} D^2 \frac{j_>}{2j+1} \ln\Delta^{-1} , \tag{2.7}$$

where

$$\Delta = \tfrac{1}{4}(\delta^2/D) . \tag{2.8}$$

We see that for $\theta \lesssim \theta_1$ the adiabatic approximation is valid for transitions with $|\Delta j| = 1$ only for

$$\theta \gg \delta/D^{1/2} = \theta_0 . \tag{2.9}$$

Finally, we also note that it is possible to estimate the angular range for which the FBA is valid as[19]

$$\theta \lesssim 3/4D = \theta_2 . \tag{2.10}$$

For $\delta \ll 1$, we have $0 \ll \theta_0 \ll \theta_1 < \theta_2$, suggesting that there is no gap between the angular regions for which (1.1) is appropriate, and that for which more elaborate calculations in the FN or ARM representation may be adequate. This approximation would also appear to be appropriate in calculations of the momentum-transfer cross section, since the second term in (2.6) is a measure of the error introduced. Finally perhaps the most important result—the FN or ARM rep-

resentation may even be useful in calculations of the integrated cross section, in the form of a *correction* to (1.3) for scattering out of the forward direction. This might be written schematically

$$\sigma_I = \sigma^{\mathrm{FBA}} - \left(\int_\theta^\pi d\sigma^{\mathrm{FBA}} - \int_\theta^\pi d\sigma^{C} \right), \tag{2.11}$$

where θ is chosen such that $\theta_0 \ll \theta \ll \theta_2$, with the first term given by (1.3), the second using (1.1) or (1.4), and the third using the result of some calculation in the FN or ARM representation. The term in large parentheses in (2.11) will be referred to henceforth as $\Delta\sigma_I$.

These arguments have several interesting consequences which can be easily tested by calculations. For example, the difference between total (summed over all final rotor states) integrated cross sections calculated in the complete representation and the result given by (1.3) should be insensitive to the initial rotor state chosen, and should agree with results for this difference obtained in the FN representation. The same should also apply to total differential cross sections for scattering out of the forward direction and total momentum-transfer cross sections. Partial cross sections calculated in the complete and ARM representations should also agree.

It should be clearly understood that these are not statements about the *accuracy* of results which might be obtained from any particular calculation, since this may depend critically on the sophistication of the scattering formalism adopted, on the accuracy with which the interaction potential is represented, and, of course, on the degree to which the conditions for the validity of the adiabatic approximation are satisfied.

In Sec. II B we will summarize the results of recent theoretical and experimental results for the alkali-metal halides, with particular attention to this issue. We conclude here by noting that for the extreme case of LiF, we obtain (see Sec. III D 5) from (2.3)

$$\delta(\mathrm{LiF}) \simeq 1.34 \times 10^{-4} T^{1/2}/E, \tag{2.12}$$

where T (°K) is the rotational temperature of the molecules and E (eV) is the energy of the incident electron. Thus for typical crossed-beam measurements ($T \sim 1000$ °K) we have $\delta \lesssim 4 \times 10^{-3}$ and $\theta_0 \lesssim 0.2°$ for $E > 1$ eV. Since from (2.10) we also have $\theta_2 \simeq 17°$, the alkali-metal halides would appear to be particularly suited to application of the adiabatic approximation.

B. Discussion of recent calculations

We first summarize the calculations which have been made according to the categories outlined above.

The most elaborate calculations in the complete representation were made by Allison[20] for CsF with $j = 41$, using a cut-off dipole potential and the close-coupling (CC) formalism. Similar calculations were made by Itikawa, who employed cut-off dipole and quadrupole potentials in a detailed study[21] of CsF with $j = 0$ and 1, and who also made a general study of the dependence of momentum-transfer cross sections on dipole moment.[22] Smith and co-workers[23,24] used semiclassical perturbation theory (SPT) for the dipole interaction to approximate the quantum-mechanical S matrix, and obtained results for a wide range of values of the dipole moment, initial rotational state, and ratio of electron energy to rotational spacing. A modified form of the FBA (MFBA) in which a hard sphere was substituted for the singular $1/r^2$ dipole potential at small radii was used by Rudge[25] in a general study for several alkali-metal halides with values of j typical of the experimental measurements. Calculations have also been made for KI (with $j = 75$) in the distorted-wave (DW) approximation using a dipole potential modified semiempirically at small radii.[12] First-order time-dependent perturbation theory (TDPT) was applied by Dickinson and Richards[26] to obtain simple formulas for integrated rotational excitation and deexcitation cross sections as a function of dipole moment, initial rotational state, rotational spacing, and approximate molecular size.

The ARM representation was employed by Takayanagi,[27] and by Ashihara *et al.*,[28] in calculations using the Glauber formalism. In his work, Takayanagi considered only $j = 0$, and the point-dipole potential. Ashihara *et al.* also investigated the effects of the quadrupole potential, induced polarization, short-range interactions (through the device of the charge distribution of the molecule in the united-atom limit), and the dependence on j. Onda[29] explicitly solved the equations for elastic scattering by a fixed dipole cut off at small radii in a study of CsCl with $j = 0$. We will for convenience refer to this model henceforth as exact adiabatic (EA).

Calculations in the FN representation were carried out by Fabrikant,[30] using essentially the same formalism as Onda, and by Dickinson[31] using classical perturbation theory (CPT). In both cases total integrated cross sections were also obtained as discussed in Sec. II A, in terms of $\Delta\sigma_I$.

The most striking result of all these calculations is that none yielded values for the total integrated cross section which differed from that given by (1.3) by more than about 20%, in sharp contrast

to the large differences obtained by Stern and co-workers. The results of these calculations are, in addition, in excellent mutual agreement for a given value of j, confirm the expected strong dependence on j (cf. the work of Rudge[25]), and also suggest that the correction $\Delta\sigma_I$ to the FBA result is quite insensitive to j, in agreement with the arguments above. This latter point was first noted by Dickinson,[31] and is supported by the results of other model studies.[20,21,23,26] Further evidence in support of this point will be presented in Sec. V. We also consider the model dependence (both collisional and potential approximations) of partial integrated cross sections with $|\Delta j| \neq 1$, and find that the results support Garrett's conclusion that they are much more model dependent than is the total integrated cross section or that for $|\Delta j| = 1$. Finally, we pursue in detail a suggested[28] resolution for the discrepancy between the calculated and measured total integrated cross sections, which raises a serious question about the credibility of the latter.

With regard to momentum-transfer cross sections, the results of the various calculations qualitatively confirm, with one exception, the experimental observation that large reductions from the FBA are obtained. One very valuable insight gained from these calculations is that this large reduction occurs in spite of significant contributions, typically two-thirds of the total, from transitions with $|\Delta j| \neq 1$. The most detailed evidence for this is given in the work of Itikawa[21,22] and Hickman and Smith,[24] but was suggested by the magnitude of the contribution to angular distributions obtained earlier.[27-29] Since only the dipole potential was included in most of these calculations, they also show that the effect is owing largely to second-order coupling of rotational states with $|\Delta j| \neq 1$ by the dipole potential.

The results of these various calculations are, however, extraordinarily diverse quantitatively. The major cause of this diversity is differences in the scattering formalism adopted and the treatment of the interaction potential. The semiclassical,[24] modified FBA,[25] classical,[31] and Glauber[27,28] calculations are not expected to be very accurate for scattering at angles $\gtrsim 60°$, which makes a significant contribution to the momentum-transfer cross section. The differences between the two adiabatic calculations[21,30] can probably be attributed to the different approaches to the solution of otherwise identical equations. The differences between the CC calculations,[20,21] and between these and the adiabatic calculations,[21] are harder to rationalize, and one is tempted to conclude[21] that this is evidence of the breakdown of the adiabatic approximation. The semiclassical[24] calculations also suggest that there is a significant dependence of the total momentum-transfer cross section on j for small j and δ, and hence that the adiabatic approximation is invalid. We will present evidence to the contrary in Sec. V.

Turning finally to differential cross sections, the results of the various calculations, again with one exception, agree qualitatively with the experimental observation that the FBA prediction is much too large except in the forward direction. They also show,[21,27-29] as stated above, that there is a very significant contribution to the total differential cross section at large scattering angles from transitions with $|\Delta j| \neq 1$; and that large-angle scattering is very sensitive to the collision approximation and to the form of the interaction potential adopted.[21,29,31] Finally, it has been well established[21,27-29,31] that the pronounced minima in the experimental results[8-11] at 60°–80° cannot be reproduced in the total differential cross section, even though they appear[20,21,25,27-29] in the partial differential cross section for transitions with $|\Delta j| = 1$. All of these results are confirmed by our own work, as will be seen.

We also provide evidence tending to confirm the suggestion[9] that "the (observed) cross sections zeros at ~80° and 180° may be artifactual; a result of the finite flexibility of the models" used to analyze the experimental data. This evidence also suggests that the experimental data, if not the cross sections extracted therefrom, may not, in fact, be inconsistent with theoretical results.

The one exception mentioned above is the results of measurements and distorted-wave calculations for KI,[12] which differed from the FBA predictions for both the differential and momentum-transfer cross sections by very much less than the results of any other measurement or calculation. It has been suggested[31] that the calculations perhaps suffered from violation of unitarity, but if so it should also have been apparent in the earlier calculations[25] which employed a similar perturbative approximation. Nevertheless, we will show in Sec. V that the use of the identical model potential in the close-coupling formalism leads to results for the differential and momentum-transfer cross sections which are drastically different, and in much better qualitative agreement with expectation. We will also consider the normalization of the measurements.

In general, while the results of model studies such as those cited in this section, and reported in Sec. V, can contribute to the resolution of important issues, such as the validity of the FBA

and the adiabatic approximation, which do not depend critically on the short-range interaction, the quantitative accuracy of the results can be questioned. The present detailed calculations for LiF also discussed in Sec. V are aimed at beginning to fill this void, and show that careful attention to the scattering formalism and accurate representation of the *total* interaction potential is of much greater importance than any issue associated with the adiabatic approximation if accurate results are wanted for anything other than the total integrated cross section or the differential cross section for scattering at small angles.

III. COLLISION FORMULATION

In all of our calculations we make the following simplifying assumptions: (i) the Born-Oppenheimer approximation in which the target molecular wave function separates into electronic, vibrational, and rotational components; (ii) the molecule confined to its ground electronic and vibrational state; (iii) the rigid-rotor approximation in which the nuclei of the molecule are fixed at the equilibrium separation. With these assumptions the equation for the scattered electron for an arbitrary coordinate system can be written

$$[T(\vec{R})+H_{\rm rot}(\hat{r})+V(\vec{R},\hat{r})-\tfrac{1}{2}k^2]\Psi(\vec{R},\hat{r})=0\,, \qquad (3.1)$$

where $\vec{R}$ is the position of the electron from the center of mass (c.m.) of the molecule, k^2 is its energy, $H_{\rm rot}(\hat{r})$ is the rotational Hamiltonian of the molecule with $\hat{r}$ describing the orientation of the molecule, and $V(\vec{R},\hat{r})$ is the potential operator.

If we further neglect exchange between the scattered and molecular electrons, we can write $V(\vec{R},\hat{r})\Psi(\vec{R},\hat{r})$ as

$$V_S(\vec{R},\hat{r})\Psi(\vec{R},\hat{r})=\langle\phi_{e,v}|V_{\rm int}|\phi_{e,v}\rangle\Psi(\vec{R},\hat{r}), \qquad (3.2)$$

where $\phi_{e,v}$ represents the electronic and vibrational components of the molecular wave function and $V_{\rm int}$ is the electronic potential between the scattered electron and molecular electrons and nuclei. We will return to the question of exchange in Sec. III D 2, and incorporate exchange effects by adding a *local*, energy-dependent effective potential to the static potential $V_S(\vec{R},\hat{r})$.

A. Reference frames

We will next discuss the two coordinate frames used in obtaining solutions to (3.1), the so-called space-fixed (SF) and body-fixed (BF) frames.

1. Space-fixed frame

In this frame the electron position $(\vec{R})$ and molecular orientation $(\hat{r})$ are referred to a set of axes fixed in space at the c.m. of the molecule. We can expand $\Psi(\vec{R},\hat{r})$ in terms of the vector-coupled product functions

$$\mathcal{Y}^{JM}_{jl}(\hat{R},\hat{r})=\sum_{m_j m_l} C(jlm_j m_l|JM)\,Y_{jm_j}(\hat{r})\,Y_{lm_l}(\hat{R})\,, \qquad (3.3)$$

where $C(jlm_jm_l|JM)$ is the Clebsch-Gordan coefficient,[32] and $Y_{jm_j}(\hat{r})$ and $Y_{lm_l}(\hat{R})$ are the eigenfunctions of $H_{\rm rot}(\hat{r})$ and the angular momentum operator $\hat{l}^2$ for the incident electron, respectively. With this expansion in (3.2), (3.1) reduces to the infinite set of coupled equations[33]

$$\left(\frac{d^2}{dR^2}-\frac{l'(l'+1)}{R^2}+k^2_{jj'}\right){}^{J}f^{jl}_{j'l'}(R) = 2\sum_{j''l''}{}^{J}V^{j'l'}_{j''l''}(R)\,{}^{J}f^{jl}_{j''l''}(R) \qquad (3.4)$$

for the radial function ${}^{J}f^{jl}_{j'l'}(R)$, where

$$k^2_{jj'}=k^2+[j(j+1)-j'(j'+1)]B \qquad (3.5)$$

is the channel energy, B is the molecular rotational constant, and

$${}^{J}V^{j'l'}_{j''l''}(R)=\langle\mathcal{Y}^{JM}_{j'l'}|V_S|\mathcal{Y}^{JM}_{j''l''}\rangle\,. \qquad (3.6)$$

The set of Eqs. (3.4) is block diagonal in J, and we will henceforth drop the superscript J on f and V. For a given value of J each value of j has associated with it all values of l which satisfy the relation $|J-j|\le l\le|J+j|$. The boundary conditions which must be satisfied by $f^{jl}_{j'l'}(R)$ are

$$f^{jl}_{j'l'}(0)=0 \qquad (3.7)$$

and

$$f^{jl}_{j'l'}(R)\underset{R\to\infty}{\sim}\delta_{jj'}\delta_{ll'}\exp[-i(k_{jj}R-\tfrac{1}{2}l\pi)] -\left(\frac{k_{jj}}{k_{jj'}}\right)^{1/2}{}^{J}S^{jl}_{j'l'}\exp[i(k_{jj'}R-\tfrac{1}{2}l'\pi)]\,.$$

The $\underline{S}$-matrix elements obtained from (3.7) define cross sections in the complete representation.

2. Body-fixed frame

In this frame the z axis of the coordinate system is oriented along the internuclear axis and therefore rotates with the molecule. The states are labeled by the quantum numbers J, l and the projection m_l of $\vec{l}$ (now referenced to the BF axis) on the internuclear axis. The various l values are coupled by $V_S(\vec{R},\hat{r})$ and the various m_l

values are coupled by $H_{\rm rot}(\hat{r})$. Since the BF and SF frames are related by a simple rotation, the collision formalism is, at this point, identical in the two frames.[34] If we make the adiabatic approximation, and neglect $H_{\rm rot}(\hat{r})$ in (3.1), $\Psi(\vec{R},\hat{r})$ can be expanded in terms of eigenfunctions $Y_{lm_l}(\hat{R})$ of $\hat{l}^2$. This leads to the infinite set of coupled equations[35,36]

$$\left(\frac{d^2}{dR^2} - \frac{l'(l'+1)}{R^2} + k^2\right) {}^{m_l}g^{l}_{l'}(R) = 2\sum_{l''} {}^{m_l}V^{l'}_{l''}(R)\,{}^{m_l}g^{l}_{l''} \quad (3.8)$$

for the radial function ${}^{m_l}g^{l}_{l'}(R)$, where

$${}^{m_l}V^{l'}_{l''}(R) = \langle Y_{l'm_l}|V_S|Y_{l''m_l}\rangle . \quad (3.9)$$

Since $H_{\rm rot}(\hat{r})$ has been neglected, the set of Eqs. (3.8) is block diagonal in m_l and is independent of $\hat{r}$, and we will henceforth drop the superscript m_l on g and V. The convention is to let m_l designate the symmetry of the total system, e.g., $m_l = 0$ is said to be Σ symmetry, $m_l = 1$, Π symmetry. A given value of m_l has associated with it all values of $l \geq |m_l|$.

The boundary conditions which must be satisfied by $g^{l}_{l'}(R)$ are

$$g^{l}_{l'}(0) = 0 \quad (3.10)$$

and

$$g^{l}_{l'}(R) \underset{R\to\infty}{\sim} \delta_{ll'}\exp[-i(kR - \tfrac{1}{2}l\pi)] - {}^{m_l}S^{l}_{l'}\exp[i(kR - \tfrac{1}{2}l'\pi)] .$$

Henceforth all references to the BF frame in this paper should be taken to imply the additional adiabatic approximation. The $\underline{S}$-matrix elements obtained from (3.10) can then be used to calculate cross sections in either the ARM or FN representation.

B. Collisional approximations

Two methods are used to obtain solutions to (3.4) and (3.8): the close-coupling approximation and the Born approximation.

1. Close-coupling approximation

This is a well-known technique for obtaining accurate, but approximate, solutions to the infinite sets of coupled equations (3.4) and (3.8) by truncating the expansions of $\Psi(\vec{R},\hat{r})$ after a finite number of terms. The approximation is valid provided that the effect of neglected channels on the cross section of interest is small. This has been shown[37] to hold rigorously "for low-energy molecular scattering below the thresholds for vibrational and electronic excitation channels even in the presence of long-range dipolar fields."

In the SF frame[33] we include all rotational states $j = 0$ to $j = j_{\max}$, and hence the number of channels for a given value of J consists of all sets of (jl) such that $j \leq j_{\max}$ and $|J - j| \leq l \leq |J + j|$. In the BF frame[38] we include, for a given value of m_l, all values of l such that $|m_l| \leq l \leq l_{\max}$. The choices of $j_{\max}$ and $l_{\max}$ may be a function of J and m_l, respectively, and are determined by the accuracy demanded of the results. If applied carefully, with large enough values of $j_{\max}$ and $l_{\max}$, cross sections of very high accuracy can be obtained.

2. Born approximation

As discussed in Sec. II, the Born approximation not only yields qualitatively, and sometimes quantitatively, accurate results for various cross sections, but also is essential in representing the effects of high partial waves in more elaborate calculations. We employ three forms of the Born approximation—the FBA and two unitarized versions.

The transition matrix in the FBA, which we will designate BI, can be written $\underline{T} = -2i\underline{B}$, where the elements of $\underline{B}$ are in the SF frame[39]

$${}^{J}B^{jl}_{j'l'} = -2i(k_{jj}k_{jj'})^{1/2}\int_0^\infty dR\,R^2 j_l(k_{jj}R)\times V^{jl}_{j'l'}(R)j_{l'}(k_{jj'}R) \quad (3.11)$$

and in the BF frame[40]

$${}^{m_l}B^{l}_{l'} = -2ik\int_0^\infty dR\,R^2 j_l(kR)\,V^{l}_{l'}(R)j_{l'}(kR), \quad (3.12)$$

where $j_l(x)$ is the spherical Bessel function of order l. We expect the $\underline{T}$-matrix elements from the BI approximation to be more accurate for higher partial waves (large l) since the centrifugal barrier will be large enough to prevent them from penetrating the region of strong potential.[41] We will denote by l^B that value of l such that for l or $l' > l^B$ the formulas (3.11) or (3.12) yield $\underline{T}$-matrix elements in good agreement with the results of close-coupling calculations for the full potentials. The choice of l^B determines some corresponding value of J^B (for $j = 0$, $J^B \simeq j_> + l^B$, where $j_>$ is the largest value of j' required in the calculations), and of $|m_l^B| = l^B$.

For strongly polar molecules the BI $\underline{T}$-matrix elements for low values of l may not satisfy the unitarity constraint. We consider the results of two modifications of the FBA which remedy this

defect. The $\underline{T}$ matrices in these two approximations, designated BII and BIII, are defined in terms of the BI matrices $\underline{B}$ by[15]

$$\underline{T}_{\mathrm{BII}} = -2i\underline{B}(1 - i\underline{B})^{-1} \tag{3.13}$$

and

$$\underline{T}_{\mathrm{BIII}} = 1 - \exp(2i\underline{B}). \tag{3.14}$$

The BII approximation can be derived alternatively from a variational prescription,[42] or from consideration of only the "on-the-energy-shell" transitions in a general transition-operator formulation.[43] The BIII approximation can, on the other hand, be identified with the near-classical limit of the collision process.[44]

These approximations not only satisfy the requirement of unitarity, but also allow some account to be taken of second-order interactions ($|\Delta j|$, $|\Delta l| \neq 1$) not allowed for in the BI approximation. Itikawa has shown,[39] for example, that the BII approximation yielded quite good results for the high partial-wave contributions to elastic scattering in CN, for which violation of unitarity was not an issue.

C. Frame transformation

We argued in Sec. II that the adiabatic approximation may be perfectly adequate for cross sections for momentum transfer and for scattering out of the forward direction. We also know that forward scattering and integrated cross sections would diverge if calculated entirely from solutions of (3.8). In order to obtain results for these cross sections we must take into account the rotational Hamiltonian. We note, however, that the BF frame equations (3.8) involve many fewer scattering channels than the corresponding SF frame equations (3.4), and are thus computationally much easier to handle. We would, therefore, like to take advantage of this computational efficiency, when it can be done *with no significant sacrifice in accuracy*. The frame transformation allows us to do this.

As noted earlier, the SF and BF frames are related by a simple rotational transformation. For the scattering matrix elements this can be written[34]

$$^{J}S^{jl}_{j'l'} = (-1)^{l+l'} \sum_{m_l} C(Jl' - m_l m_l \,|\, j'0) \times {}^{m_l}S^{j}_{l'}\, C(Jl - m_l m_l \,|\, j0). \tag{3.15}$$

The $\underline{S}$-matrix elements $^{J}S^{jl}_{j'l'}$ obtained from (3.15) with $^{m_l}S^{j}_{l'}$ defined by (3.10) are, as a consequence of the adiabatic approximation, not strictly equivalent to those defined by (3.7). Cross sections obtained from these $\underline{S}$-matrix elements are in the ARM representation.

The conventional application[45] of the frame-transformation theory has been to divide the calculation into two regions of space at R_t, which is characteristic of the molecular size. For $R \leq R_t$, where the strong short-range interaction potential dominates, the calculations are performed in the BF frame. The wave functions so obtained are then transformed at R_t to the SF frame. The calculations are then continued for $R \geq R_t$ in the SF frame using (3.4). This approach yields results which are not, strictly speaking, in either the complete or ARM representation, but a mixture of both.

In the most detailed calculations on LiF reported here we employ an alternative approach which is computationally more efficient. It consists, quite simply, of using the BF frame equations (3.8) for partial waves with small l, and the SF frame equations (3.4) for partial waves with large l. The specific meaning of "small" and "large" in this context will become clearer in what follows, and will be specified explicitly in Sec. IV C.

The justification for this procedure is provided by a simple extension of the arguments presented in Sec. II with regard to the validity of the adiabatic approximation. The essential requirement is that all interactions—kinetic, rotational, potential—that make a significant contribution to the *total* distortion of the wave function of the scattered particle must be included in the scattering equations. This is a much less restrictive condition than that implicit in the usual application of the frame transformation, viz., that all interactions must be included which are comparable, in any given region of space, to the dominant interaction.

We can see why the latter might be unnecessarily restrictive by considering the relative contributions, as well as relative strengths, of the kinetic, potential, and rotational energy components as a function not only of distance from the c.m. of the molecule, but also as a function of l. For small l the wave function for the scattered particle will penetrate deeply into the molecular charge cloud, and its properties will be determined primarily by the strong short-range interaction potential. The additional accumulation of phase owing to the rotational Hamiltonian will be small by comparison, and may be neglected, despite the fact that at some large radii the rotational and kinetic contributions may be comparable.

For large l, however, the wave function for

the scattered particle is confined to the region outside the molecular charge cloud, and its properties are primarily determined by the long-range component of the potential energy, which may be comparable to the rotational contribution. The accumulation of phase from large radii owing to the rotational Hamiltonian may be a significant part of the total, and cannot, therefore, be neglected. Conversely, the contribution from the strong potential at short distances is small and may be very crudely approximated, e.g., by the FBA for the point dipole in the limit of very large l. The actual validity of these approximations must, of course, be tested in particular applications, just as the value of R_t must be carefully chosen in the conventional application of the frame transformation.

This suggests, then, that some value l^T can be specified such that for l and $l' \leq l^T$ the elements ${}^J S^{jl}_{j'l'}$ can be obtained with requisite accuracy from close-coupling calculations performed completely in the BF frame, with particular attention to an accurate representation of the short-range interaction, and application of (3.15). For l or $l' > l^T$ the elements ${}^J S^{jl}_{j'l'}$ may be obtained either from close-coupling solutions of (3.4) with a model potential which accurately represents only the long-range interaction, or for l or $l' > l^B$ (see Sec. III B 2) from the FBA formula (3.11). From the form of (3.15) it follows that close-coupling calculations in the BF frame are only required for $m_l \leq l^T$. For a particular choice of initial rotor state j these calculations are sufficient to completely specify the elements ${}^J S^{jl}_{j'l'}$ for all l and $l' \leq l^T$, all J satisfying $|j-l| \leq J \leq |j+l|$, and all j' satisfying $|J-l'| \leq j' \leq |J+l'|$. If, for example, we choose $l^T = 4$ and are interested in transitions involving the ground rotor state ($j=0$), BF frame calculations with $m_l^T \leq 4$ specify all elements ${}^J S^{jl}_{j'l'}$ with l and $l' \leq 4$, $0 \leq J \leq 4$, and $0 \leq j' \leq 8$.

In the present calculations we actually do something slightly different but practically equivalent. Since we are interested in transitions involving the ground rotor state, we choose some value J^T and carry out calculations in the BF frame sufficient to specify the elements ${}^J S^{jl}_{j'l'}$ for all $J \leq J^T$ and all $j' \leq j^s$, where j^s is the highest rotor state of interest. We require, therefore, calculations in the BF frame for $m_l \leq m_l^T = J^T$ which have $l_{\max}$ not less than $J^T + j^s$ (see Sec. III B 1). Elements for values of $J > J^T$ are obtained as outlined in the previous paragraph, with model-potential calculations used for $J^T < J \leq J^B$ and the FBA formula (3.11) used for $J > J^B$. The specific choice of J^T depends, of course, on the accuracy required, and the sensitivity of the results to the value chosen must be carefully checked. We will refer to cross sections obtained in this way as being in the complete representation, although strictly speaking, the ARM representation is being used for $J \leq J^T$.

In order to test this technique we performed fully converged close-coupling calculations in both the SF and BF frames at several energies with the static surface [S(36), see Sec. III D 1]. Applying the frame transformation (3.15) to the BF frame $\underline{S}$-matrix elements, we found that results obtained for the lowest few quantum numbers $(j, l, J \leq 4)$ agreed with SF frame $\underline{S}$-matrix elements to better than 1%. Roughly equivalent values of $l_{\max}$ were required for convergence in the BF and SF frames, but the latter also required $j_{\max} \sim 20$. Large-scale calculations in the SF frame for low values of J with the number of total scattering channels implied by these values of $j_{\max}$ and $l_{\max}$ are clearly impractical at present.

D. Potential-energy surfaces

In this section we describe the procedure we employ for calculating the matrix elements (3.6) and (3.9). In addition, we describe a method for incorporating exchange effects (which we neglected earlier) into the formulation by augmenting the static surface by a local, energy-dependent effective-exchange potential. Polarization effects are included by a semiempirical adiabatic polarization potential. Finally, we discuss several model potentials, some of which have been used in previous polar-molecule calculations.

1. Static surface

We represent the electronic wave function for the N-electron, closed-shell target molecule as a single-configuration Hartree-Fock function of the form[38,46]

$$\Phi_e(1\cdots N) = \frac{1}{\sqrt{N!}} \sum_{\alpha\cdots\pi} \epsilon_{\alpha\cdots\pi}\, \phi_\alpha(1)\cdots\phi_\pi(N), \tag{3.16}$$

where $\phi_i(j)$ represents the ith spin-orbital at position $\vec{s}_j$, $\epsilon_{\alpha\cdots\pi}$ the Levi-Civita density, and where the sum over each index $\alpha\cdots\pi$ runs from 1 to N. Substituting this expression into (3.1), we find that $V_S(\vec{R},\hat{r})$ for an electron interacting with an N-electron target molecule is given by

$$V_S(\vec{R},\hat{r}) = V_n(\vec{R},\hat{r}) + V_e(\vec{R},\hat{r}), \tag{3.17}$$

where

$$V_n(\vec{R},\hat{r}) = -\sum_\gamma \frac{Z_\gamma}{|\vec{R}-\vec{R}_\gamma|}, \tag{3.18}$$

with the sum over all nuclei of charge Z_γ and position $\vec{R}_\gamma$ relative to the c.m. of the molecule, and

$$V_e(\vec{R},\hat{r}) = 2\sum_{j=1}^{N_{oc}} \int \phi_j^*(\vec{s}) \frac{1}{|\vec{R}-\vec{s}|} \phi_j(\vec{s})\, d\vec{s}\,, \qquad (3.19)$$

with $\vec{s}$ the coordinates of electrons in spin-orbital j relative to the c.m. of the molecule and $N_{oc} = \frac{1}{2}N$ the number of occupied orbitals. We have therefore divided the static potential into its nuclear and electronic components, V_n and V_e, respectively.

In order to simplify the angular integration implicit in the matrix elements (3.6) and (3.9), we expand (3.17) in a Legendre series as

$$V_S(\vec{R},\hat{r}) = \sum_{\lambda=0}^{\infty} v_{n,\lambda}(R) P_\lambda(\cos\theta) + \sum_{\lambda=0}^{\infty} v_{e,\lambda}(R) P_\lambda(\cos\theta)\,, \qquad (3.20)$$

with $\hat{r}\cdot\hat{z} = \cos\theta$ for $\hat{z}$ the coordinate axis of the SF or BF frame. We can now perform the angular integrations analytically. In either frame, the resulting expression is proportional to the product of several Clebsch-Gordan and/or Racah coefficients.[47]

The sums in (3.20) must be truncated at some finite values λ_e and λ_n of λ, and we define $\lambda_{max} = \max(\lambda_e, \lambda_n)$. It should be noted that since higher components of v_λ couple higher terms in the wave-function expansion, the number of terms in both expansions must be increased *simultaneously* until satisfactory convergence in the results is achieved. The nuclear component $v_{n,\lambda}(R)$ has a simple analytical form in this single-center expansion,[40] while the electronic component must be determined by numerically integrating[48] (3.19). On the other hand, far fewer electronic (λ_e) than nuclear (λ_n) components are needed to accurately represent that contribution to the total surface.[49] This results from the fact that the electronic component represents the interaction between an electron and the diffuse electronic charge cloud of the molecule, while the nuclear component in (3.20) is an attempt to represent a singular potential with a nonsingular expansion. The value of λ_{max} required for convergence is thus determined by the first sum in (3.20), and we will henceforth denote the static surface so defined as $S(\lambda_{max})$.

2. Exchange

We have so far neglected exchange effects in order to simplify the scattering equations. However, it is well known that exchange plays an important role in low-energy electron-molecule collisions.[14,50] The proper inclusion of the exact nonlocal energy-dependent exchange potential in (3.1) would be extremely difficult for highly polar molecules. Recently, however, several *local*-exchange model potentials have been shown to give quite good results for electron-molecule collisions at low and intermediate energies. The advantage of a local potential is that it can be appended directly to V_s in (3.17) without any change in our previous formulation.

We employ the local, energy-dependent free-electron-gas[51] (FEG) exchange potential of the form[35]

$$V_{FEG}(\vec{R},\hat{r}) = -(2/\pi)k_F F(\eta)\,, \qquad (3.21)$$

where

$$F(\eta) = \frac{1}{2} + \frac{1-\eta^2}{4\eta} \ln\left|\frac{1+\eta}{1-\eta}\right|, \qquad (3.22)$$

$$\eta = \kappa/k_F\,, \qquad (3.23)$$

$$k_F = [3\pi^2 \rho(\vec{R})]^{1/3}\,, \qquad (3.24)$$

and

$$\kappa^2 = k^2 + 2I_P + k_F^2\,, \qquad (3.25)$$

with I_P the molecular ionization potential and $\rho(\vec{R})$ the molecular charge density. This formula arises from treating the molecular electrons as a FEG and the incident electron in the Born approximation. The FEG charge density is replaced by the actual molecular change density of the target molecule determined from (3.16). In addition, the local momentum κ has been improved by including the incident momentum of the scattered electron k and the ionization potential of the molecular valence electron.

The static-exchange (SE) potential-energy surface is given by

$$V_{SE}(\vec{R},\hat{r}) = V_S(\vec{R},\hat{r}) + V_{FEG}(\vec{R},\hat{r})\,. \qquad (3.26)$$

As with the static surface, the exchange potential energy is expanded in a Legendre series as

$$V_{FEG}(\vec{R},\hat{r}) = \sum_{\lambda=0}^{\infty} v_{ex,\lambda}(R) P_\lambda(\cos\theta) \qquad (3.27)$$

which is truncated at a finite value λ_{ex} of λ. For all work described here we found that the adequate convergence could be obtained with the same number of terms (λ_{ex}) in the expansion (3.27) as in the expansion of the electronic part of V_S.

The success of the FEG models in accurately representing, through a local potential, the more important features of the nonlocal exchange terms has been well documented.[46,49,51,52] Studies using several local-exchange model potentials have been made[46,49] for electron collisions with H_2, N_2, and CO_2. The results, when compared with

those from calculations employing more rigorous representations of the exchange effect, and with measurements, have been most encouraging. The particular model described by (3.21)–(3.25), referred to as the Hara FEG exchange potential (HFEGE) since first used by Hara in studies of e-H_2 collisions,[35] seems most appropriate for *low*-energy electron collisions with many-electron targets.

3. Polarization

The use of a wave function for a ground-state isolated molecule in the derivation of the interaction potential does not take into account the polarization effects that arise from the distortion of the molecular charge cloud in response to the incident electron. We will investigate the effect of this omission by adding to the potential-energy surface an effective, adiabatic polarization potential of the form

$$V_{\rm pol}(\vec{R},\hat{r}) = -[\alpha_0 + \alpha_2 P_2(\cos\theta)]\, C(R)/2R^4, \quad (3.28)$$

where

$$C(R) = 1 - \exp[-(R/R_c)^6]. \quad (3.29)$$

The spherical and nonspherical components of the dipole polarizability of the molecule are given by α_0 and α_2; the cut-off radius R_c is chosen within the constraint that the polarization potential has negligible strength within the molecular charge cloud. Thus, the static-exchange-polarization (SEP) surface is given by

$$V_{\rm SEP}(\vec{R},\hat{r}) = V_{\rm S}(\vec{R},\hat{r}) + V_{\rm FEG}(\vec{R},\hat{r}) + V_{\rm pol}(\vec{R},\hat{r}). \quad (3.30)$$

Calculations for several molecules (N_2, CO_2, CO), where polarizabilities are well known and for which resonance features in a particular symmetry had been observed experimentally were improved by varying R_c in (3.29) until the calculations gave a resonance at the experimental position.[38,40,46,49,53] The integrated and momentum-transfer cross sections obtained, which away from the resonance depended on many symmetries in addition to that in which the resonance appeared, were found to be in quite good agreement with measurements over a large energy range. The "tuning" procedure therefore appeared to give an improved total-potential-energy surface for the collision. For the alkali-metal halides that we consider, the polarizabilities are not well known and as yet there is no direct experimental evidence for any resonance features. Therefore, we include the polarization surface in our calculations only to judge the sensitivity of the features we observe in the SE calculations to a "reasonable" choice of polarization interaction.

4. Model potentials

The SEP surface was used only for calculations on LiF, and the S and SE surfaces for calculations on LiF, LiCl, NaF, and NaCl. For LiF, and for KI and CsF, we also perform collision calculations using a number of much simpler model potentials. The first of these potentials is the point dipole (PD) which has the form

$$v_1(R) = -D/R^2, \qquad v_\lambda(R) = 0, \quad \lambda \neq 1. \quad (3.31)$$

This particular model is used only in Born-approximation calculations. The second set of model potentials that we employ is the cut-off dipole model [DCO(R_0)] which has the form

$$v_1(R) = -(D/R^2)\{1 - \exp[-(R/R_0)^6]\}, \qquad v_\lambda(R) = 0, \quad \lambda \neq 1. \quad (3.32)$$

This model has been used extensively in calculations of electron-polar molecule collisions,[54] and is simply the PD model cut off within the molecular charge cloud to avoid the unphysical dipole singularity at the molecular c.m. We include studies of it here in order to determine how well it compares with more realistic surfaces (S, SE, SEP), and to investigate several qualitative aspects of the collision process. Different forms of the cut-off function (3.32) were also used in model studies for KI and CsF for direct comparison with earlier work.[12,20]

The third set of model potentials of the static surface are what we shall call truncated static models. For these models, we use the expansion coefficients of the static surface given by (3.20) but include a much smaller set of these terms than is necessary to accurately represent the full static surface. We shall present results from two such truncated models with $\lambda_{\rm max} = 2$ and 11 [S(2), S(11)] for LiF collisions. As we shall see later, no fewer than 37 ($\lambda_{\rm max} = 36$) terms are needed to describe accurately the full S and SE surfaces for LiF.

5. Molecular data

The molecular data used in the various calculations are collected in Table I. The rotational constrants and dipole moments used for LiF, LiCl, NaF, and NaCl were obtained from the equilibrium Hartree-Fock wave functions[55] used to generate the potential surfaces. The most accurate measured values[56] of B and D are also given for comparison. The entry in the third

TABLE I. Molecular data for the alkali-metal halides used in this work.

	LiF	LiCl	NaF	NaCl	KI	CsF
B [b] (hartree)	5.96(−6) [a]					
	[6.18(−6)]	[3.24(−6)]	[1.99(−6)]	[9.98(−7)]	[2.77(−7)]	[8.40(−7)]
D [b] (ea_0)	2.59	2.86	3.29	3.61		
	[2.49]	[2.81]	[3.21]	[3.54]	[4.26]	[3.10]
$\delta ET^{1/2}$ [c]	1.34(−4)	1.03(−4)	8.06(−5)	6.40(−5)	3.72(−5)	5.53(−5)
I_P (hartree)	0.472	0.376	0.426	0.348		
α_0 (a_0^3)	4.64					
α_2 (a_0^3)	1.04					

[a] The power of ten is given in parentheses.
[b] The values in [ ] are from Ref. 56.
[c] For E in eV and T in °K.

row defines δ, the figure of merit for the adiabatic approximation, as a function of molecular rotational temperature T and electron kinetic energy E. The ionization potentials were estimated from Koopman's theorem.[57] The values of α_0 and α_2 for LiF were determined from the value of $\alpha_{\parallel}$ given by McLean and Yoshimine,[55] and $\alpha_{\perp}$ estimated by scaling the value[58] of $\alpha_{\perp}$ for HF by the ratio $\alpha_{\parallel}(\mathrm{LiF})/\alpha_{\parallel}(\mathrm{HF})$, as suggested by Kolker and Karplus.[59]

IV. SCATTERING CALCULATIONS

In this section we describe in detail the procedures used to solve the sets of coupled equations (3.4) and (3.8), to extract scattering cross sections, and to fix the numerical accuracy of the results. We emphasize application to LiF, since this system was the most extensively studied. Calculations in the complete and mixed representations are limited, for computational simplicity, to elastic scattering from the ground ($j=0$) rotational state, and inelastic transitions to the lowest few excited rotational states needed to insure convergence in total cross sections.

A. Solution of the coupled equations

If N channels are retained in the expansion of the system wave function, (3.4) and (3.8) become sets of N coupled differential equations for each particular J or m_l block, respectively. The solution vector has N components or channel wave functions that satisfy the particular boundary condition (3.7) or (3.10), and there are N linearly independent solution vectors. We can therefore represent (3.4) and (3.8) in general matrix form as

$$\mathfrak{L}\underline{U}(R)=\underline{V}(R)\underline{U}(R)\,, \tag{4.1}$$

where $\mathfrak{L}$ represents the diagonal operator on the left-hand side of either (3.4) or (3.8), $\underline{V}(R)$ represents the potential-coupling term on the right-hand side of these equations, and $\underline{U}(R)$ is the matrix of solution vectors.

We convert the set of coupled differential equations (4.1) to a set of coupled integral equations of the form[60]

$$\underline{U}(R)=\underline{U}_0(R)+\int_0^{\infty} G(R,R')\underline{V}(R')\underline{U}(R')\,dR'\,, \tag{4.2}$$

where $G(R,R')$ is the Green's function satisfying

$$\mathfrak{L}G(R,R')=\delta(R-R')\,, \tag{4.3}$$

and $U_0(R)$ is a solution of the homogeneous equation. A trapezoidal quadrature is used to approximate the integrals.[61] For such an approximation, $\underline{U}(R_i)$ depends on integrals from R_1 to R_{i-1}. Therefore, $\underline{U}(R)$ can be propagated outward, noniteratively, into the asymptotic region to some $R_{\max}$ where the potential has effectively vanished.[48] The wave function is then fit to its asymptotic form (3.7) or (3.10), and the appropriate $\underline{S}$ matrix extracted.

While the various solution vectors in (4.2) are formally linearly independent, the solutions can become numerically dependent as they are propagated outward owing principally to the drastically different rates of growth of the various channel wave functions and the inherent round-off errors of the computer. We have found that by applying a stabilization technique,[62] by which $\underline{U}(R)$ is placed in upper triangular form every few integration steps, linear independence of solutions for systems with as many as 45 channels can be easily maintained.[48]

B. Evaluation of cross section

All cross sections must be evaluated, in principle, by an infinite sum over all J or m_l. For

highly polar molecules, literally hundreds of values of J might be required in order to accurately converge the integrated cross section, and fewer but still a large number for momentum-transfer and differential cross sections. In fact, as implied in Secs. IIA and IIIC, it is unnecessary to explicitly calculate $\underline{S}$-matrix elements for $J > J^{\max}$, or $m_l > m_l^{\max}$, for quite reasonable values of $J^{\max}$ or $m_l^{\max}$. One uses instead completion formulas that correct the FBA expressions (1.1)–(1.3) by a rapidly convergent sum of *differences* of quantities involving calculated $\underline{S}$-matrix elements and the corresponding BI elements from (3.11) or (3.12). A general completion formula for the differential cross section in the complete representation has been given by Crawford and Dalgarno,[63] and the analogous formula for the FN representation is easily written.

We have obtained integrated, momentum-transfer, and differential cross sections[64] by using these completion formulas, and combining the results of various close-coupling calculations. For the highly converged ($\lambda_{\max} = 36$) S, SE, and SEP surfaces $\underline{S}$-matrix elements were obtained from the BF frame calculations using the frame transformation (3.15) for $J \leq J^T$, where $J^T = m_l^T$ since we consider here only transitions from the initial rotor states with $j = 0$. These were combined with the results of calculations for the DCO(0.5) model surface in the SF frame for $J^T < J \leq J^B$, and BI $\underline{T}$-matrix elements for the PD potential from (3.11) for $J^B < J \leq J^{\max}$. These results for LiF are the primary objective of this work.

We have also obtained integrated, momentum-transfer, and differential cross sections in the complete representation using $\underline{S}$-matrix elements from close-coupling SF-frame calculations with the truncated static surfaces and several DCO model surfaces for $0 \leq J \leq J^B$, and BI $\underline{T}$-matrix elements as above. Momentum-transfer cross sections in the FN representation were obtained using $\underline{S}$-matrix elements from the SE(36) surface and several model surfaces for $0 \leq m_l \leq m_l^B$, and BI $\underline{T}$-matrix elements from (3.12) for $m_l^B < m_l \leq m_l^{\max}$. The quantity $\Delta\sigma_I$ was also obtained in the FN representation by evaluating the partial-wave analog of (2.11). Finally, we have carried out calculations in both the complete and FN representations using the BII and BIII approximations.

C. Convergence studies

In carrying out these calculations we set the goal of obtaining total integrated, momentum transfer, and differential cross sections *numerically* accurate to better than 1%, 5%, and 10%, respectively, whatever the representation, scattering approximation, or potential surface employed. To achieve this goal it was necessary to carefully check many aspects of both the scattering and cross-section calculations.

In discussing the convergence properties of the scattering calculations we emphasize here those for LiF carried out in the BF frame for the SE(36) surface, since these were the most difficult. The observations made will apply, however, equally, though generally not as strictly, to close-coupling calculations in both frames with other potential surfaces. The accuracy of the scattering calculations depends ultimately on the accuracy with which the coefficients of the Legendre expansions (3.20) and (3.27) are evaluated, and on five parameters influencing the solutions of (3.4) and (3.8): (i) size of integration mesh used to evaluate (3.19), and that used in (4.2); (ii) number of stabilizations; (iii) matching radius $R_{\max}$; (iv) number of channels N included; and (v) number of expansion terms in the potential surface.

(i) The radial integrals involved in (3.19) were evaluated with successively larger numbers of radial mesh points until satisfactory convergence was obtained in both the $v_\lambda(R)$ and cross sections. It proved to be particularly important to check the latter for energies $\lesssim 3.0$ eV. The accuracy of the quadrature scheme to evaluate the integral in (4.2) was checked in the same way. We found that a step size of $0.01a_0$ for $0.50a_0$ on either side of the nuclei was required to accurately represent the effect of the strong-nuclear-potential component of the wave function. Away from the nuclei, the step size could be increased substantially reaching $0.50a_0$ to $1.0a_0$ in the region where only the dipole term is important ($R \gtrsim 15.0a_0$).[65] Since such a fine mesh is required to accurately represent the short-range potential surface and wave function and such large steps can be taken outside this regime, usually less than 25% of the time of the calculations was expended in the region beyond $\sim 10.0a_0$.

(ii) For the number of channels of order 12 or greater, the solutions become noticeably linearly dependent. To perform calculations for a larger number of channels, we must employ the stabilization technique mentioned above. By performing stabilizations every three integration steps within the short-range ($R \lesssim 10.0a_0$) region and every six steps in the long-range ($R \gtrsim 10.0a_0$) region we could guarantee linearly independent solution vectors.

(iii) The value of $R_{\max}$ must be large enough that the potential energy is negligible and the channel wave functions are uncoupled and behaving as combinations of Bessel and Neumann functions. The procedure employed is to simply continue to step

out in R until partial integrated cross sections calculated at subsequent values of R have converged to better than 1%. R_{max} of $200.0a_0$ was found to be sufficient for incident electron energies between 1.0 and 20.0 eV. The value of R_{max} must be increased as the energy is decreased below 1.0 eV, reaching $500.0a_0$ for 0.14 eV. The large values of R_{max} that must be used to guarantee this precision in the cross section arise solely from the asymptotic behavior of the long-range dipole-moment term of the potential surface. Thus, similar values for R_{max} must be used to converge the scattering calculations with the model potentials.

(iv) and (v) The most time consuming convergence test is that for the number of terms that must be included in the expansions of the wave function and potential-energy surfaces. Since higher moments of the potential surface couple higher channels of the wave function to the lowest few channels in which we are interested, the convergence studies for the wave-function and potential-surface expansions must be treated together. The procedure we employ to determine convergence of cross sections with respect to these two quantities is as follows: (a) for a given value of l_{max} and λ_{max} the coupled equations are integrated and the cross sections determined, (b) the calculation is repeated with a larger value of l_{max} and λ_{max} until subsequent cross sections agree to within a given tolerance. This procedure guarantees "local" convergence. To guarantee a "global" convergence, the calculations are performed with six to ten channels more than the number found to give good local convergence. This procedure is necessary since the cross sections may be very slowly convergent or not yet in a monotonically convergent regime. We have found that by setting $\lambda_{max} \cong l_{max}$ and varying both simultaneously, we can very rapidly reach a regime in these quantities in which the cross sections are reasonably converged. Once this regime is reached, a finer convergence test must be employed by varying λ_{max} and l_{max} independently.

To illustrate these points, we display in Table II a portion of a convergence study for l_{max} and λ_{max}. In Table II(a), we demonstrate the technique of simultaneously varying l_{max} and λ_{max}. We present the eigenphase sum and the elastic cross section for the lowest transition ($l = 0 \rightarrow l' = 0$). We note from this table a fact observed in all our polar-molecule calculations—that for a given basis (λ_{max}, l_{max}) the $\underline{T}$-matrix elements for transitions among the lowest few partial waves ($l \lesssim 4$) are always more highly converged than the cor-

TABLE II. Convergence properties for the LiF SE(36) surface at 2.0 eV for $m_l = 0$ in the BF frame, for simultaneous (a) and independent (b) variation of λ_{max} and l_{max}. The upper entry in each row is the value of $\sigma(0 \rightarrow 0)$ (in a_0^2) and the lower entry is the eigenphase sum.

	(a)		(b)		
$l_{max} = \lambda_{max}$		l_{max}/λ_{max}	32	36	40
8	23.985 −0.3081	22		25.337 −0.3978	
10	27.163 −0.0294	26	25.417 −0.3440	25.416 −0.3364	25.417 −0.3352
12	30.591 0.2513	30	25.490 −0.3195	25.479 −0.3080	
14	36.378 0.7642	32	25.529 −0.3132	25.504 −0.3001	25.506 −0.2940
18	28.021 −0.8630	34		25.527 −0.2945	25.525 −0.2872
22	25.695 −0.4973				
26	25.514 −0.3825				
30	25.517 −0.3295				
32	25.529 −0.3132				
34	25.541 −0.3004				

responding eigenphase sum. Since it is these elements that are most important in the frame-transformation formula (3.15) for the lowest few rotational states of interest, we conclude that convergence tests based on the eigenphase sum may be overly strict for polar molecules. From Table II(a) it would appear that the basis ($l_{max} = \lambda_{max} = 26$) is adequate. In Table II(b) we present a more detailed study of the convergence properties around this choice of basis size. For considerations of economy in calculations and accuracy in the collision quantities, we selected a basis with $l_{max} = 26$ and $\lambda_{max} = 36$ ($\lambda_e = 24$).[66] This basis yielded the desired convergence over the range of incident electron energies between 1.0 and 20.0 eV. For lower energies the basis had to be increased, e.g., for 0.14 eV $l_{max} = \lambda_{max} = 42$ was required for comparable accuracy.

Before we leave a discussion of the BF convergence properties, we should mention three other points. First, for a given basis, the higher symmetries were much better converged than the Σ symmetry. While an $l_{max} = 26$ was required to converge the Σ cross sections at 2.0 eV, an $l_{max} = 18$ was adequate for convergence in the Π and higher symmetries. Second, for a given basis, the SE(36) and SEP(36) cross sections were generally better converged than the S(36) ones. Finally for the truncated static and DCO surfaces a basis of $l_{max} = 22$ was required for the lowest energies and the Σ symmetry, but $l_{max} = 16$ was adequate for higher energies and/or symmetries.

Except for comparative purposes, all close-coupling calculations in the SF frame were performed only with the truncated static and DCO model potentials. In order to obtain results of the required accuracy for transitions involving the lowest few rotational states of interest, bases of $j_{max} = 11$ and 5 were required for the S(11), and S(2) and DCO surfaces, respectively, for the lowest values of J (typically $J \leq 4$), but slightly smaller bases were adequate for larger values of J.

Turning to the generation of cross sections, we must consider the choice of the various parameters which enter: $m_l^T, m_l^B, m_l^{max}, J^T, J^B, J^{max}$, and the largest rotor state j^s and angular momenta l^s included in the sum for total cross sections. The choice of these parameters depended of course, on the particular cross section of interest as well as the accuracy required. They were also found to be mildly energy dependent, but the values chosen were adequate for the entire energy range studied. The parameters $m_l^B, m_l^{max}, l^s, J^B, J^{max}$, and j^s were, however, quite insensitive to the representation of the interaction potential.

For the most elaborate calculations carried out, those involving the highly converged ($\lambda_{max} = 36$) S, SE, and SEP surfaces and the frame transformation (3.15), we found that $m_l^T = 3$ was required, and hence $J^T = 3$.

Differential cross sections were calculated only in the complete representation, and we found that acceptable convergence was assured with $J^B = 20$. The completion formula[63] is expressed as a sum over Legendre polynomials. As a general rule we found that more than 25 moments had to be obtained accurately, and we usually calculated 28, hence $J^{max} = J^B + 28 = 48$. The behavior of the total differential cross section as a function of J^B is illustrated in Table III.

The completion formula for integrated and momentum-transfer cross sections usually used here[7] have $J^{max} = J^B$ and $m_l^{max} = m_l^B$. The results were found to agree with those obtained by integrating the differential cross section to within the required accuracy. Although most of our results for momentum-transfer cross sections in the complete representation were obtained with $J^B = 20$, yielding very accurate partial momentum-transfer cross sections, $J^B \sim 8$–12 was found to be adequate if only momentum-transfer or integrated cross sections were required, and $J^B = 10$ was used for the CsF calculations. For calculations of $\Delta\sigma_I$ and the total momentum-transfer cross section in the FN representation $m_l^B = 3$ was found to be adequate.

For total differential and momentum-transfer cross sections in the complete representation it was usually necessary to include all transitions from $j = 0$ to $j' \leq 4$, i.e., $j^s = 4$; but $j^s = 3$ was adequate for total integrated cross sections. For $\Delta\sigma_I$ and the total momentum-transfer cross section in the FN representation we included all partial waves with $l \leq 12$, i.e., $l^s = 12$. The dependence of the total momentum-transfer cross section

TABLE III. Total differential cross section (in a_0^2/sr) for the LiF SE(36) surface at 5.44 eV as a function of J^B. For the purposes of this study only, $j^s = 3$.

θ/J^B	10	20	24
15	324.78	306.87	312.88
30	51.62	53.63	54.16
45	15.63	15.55	15.67
60	6.62	6.74	6.80
75	4.17	4.41	4.48
90	3.63	3.59	3.60
105	2.72	2.86	2.81
120	1.96	2.01	1.91
135	1.36	1.39	1.31
150	1.38	1.36	1.31
165	1.85	1.76	1.73
180	2.04	1.96	1.94

TABLE IV. Total momentum-transfer cross section and $\Delta\sigma_I$ for the LiF SE(36) surface at 2.0 eV in the BF frame as a function of m_i^B and l^s.

	σ_M (a_0^2)			$\Delta\sigma_I$ (a_0^2)		
m_i^B/l^s	4	8	12	4	8	12
1	179.2	180.0	179.4	302.8	311.1	314.4
2	201.7	204.5	204.0	307.3	320.2	325.5
3	202.2	206.3	205.9	307.8	324.2	331.3

and $\Delta\sigma_I$ in the FN representation on m_i^B and l^s is illustrated in Table IV. We see that σ_M and $\Delta\sigma_I$ have similar convergence properties with respect to m_i^B, but that the latter converges more slowly in l^s. The maximum numerical error in $\Delta\sigma_I$, which occurs at the lowest energies, is estimated conservatively to be 15%.

V. RESULTS AND DISCUSSION

As stated in the Introduction, this work has several purposes. The first part of this section is devoted to discussion of model studies for two alkali-metal halides (KI and CsF) with emphasis on several qualitative aspects of the scattering process. In particular we address the question of the validity of the adiabatic approximation, and attempt to resolve several of the discrepancies between the results of earlier model studies, and between these studies and measurements. The second part is devoted to results of the detailed study of the representative highly polar molecule LiF, and includes preliminary results for three other alkali-metal halides.

A. Model studies

In these studies we have performed several close-coupling calculations for KI and CsF using DCO model potentials as defined in Sec. IIID4, with the cutoff given by (3.32) and using forms employed by other workers. Specifically, for KI and CsF we carried out calculations using the hard-sphere cut-off dipole potentials exactly as defined by Rudge *et al.*[12] and Allison,[20] respectively. For CsF we also carried out calculations using the form (3.32) with R_0 exactly as given by Itikawa.[21] The results of these calculations, which will be designated DCO(R), DCO(A), and DCO(I), respectively, can then be compared with the results of these workers with no ambiguity about the effect of the potential at short range. For KI we also carried out close-coupling calculations with the form (3.32), and with BII approximation for purposes of comparison. Finally, we have also investigated the general dependence of the momentum-transfer cross section on dipole moment with both the BII and BIII approximations.

TABLE V. Total integrated cross section for 1.0-eV electrons on CsF in initial rotor state j.

No.	j	σ_I (a_0^2)	Method [a]	Reference
1	0	12 479	BI	•••
2	0	10 406	TDPT [b]	26
3	0	11 242	CC [DCO(I)]	Present
4	0	11 233	CC [DCO(A)]	Present
5	41	8 304	BI	•••
6	41	7 032	SPT	23
7	41	6 911	MFBA	25
8	41	6 231	TDPT [b]	26
9	41	7 153	CC	20
10	~41	3 930	Expt.	9

[a] See Secs. II B and VA for notation in Tables V–VIII.
[b] Includes only transitions with $|\Delta j|=1$.

1. Integrated cross section

We first consider the total integrated cross section, illustrative results for which are given in Table V. Before discussing the calculated results in detail we first attempt to resolve the large discrepancy between the calculations and the measurement. A quite simple resolution has been suggested,[28] and we pursue it quantitatively here. Using (2.10) we would estimate that the FBA should be reasonably accurate for $\theta \lesssim 15°$ for all of the alkali-metal halides. All of the theoretical studies to date, including the present results for LiF, agree with this estimate. Using the integral of the FBA differential cross section for $\theta \leq 15°$ as a rough estimate of the lower limit for the total integrated cross section we obtain results which are significantly larger than the measured results over much of the energy range. This is illustrated in Fig. 1 for CsF.

Using the FBA even more conservatively, for CsF, CsCl, and KI under the experimental conditions approximately (40–50)% and (50–60)% of the total integrated cross section comes from the first 1° and 2°, respectively, for electron energies in the range 1–10 eV. The values of this ratio are quite insensitive to the value of j, and hence to averaging over the actual experimental distribution of rotational states. At the lowest energies the contribution for $\theta \leq 2°$ even exceeds the measured results for all three alkali-metal halides. The analysis of the experimental data appears to have used a model[9] of the differential cross section which deviates significantly from the FBA even "at center-of-mass angles less than 2° where experimental data are lacking" (cf. Fig. 11 in Ref. 9). There is no justification, either experimental or theoretical, for such a model.

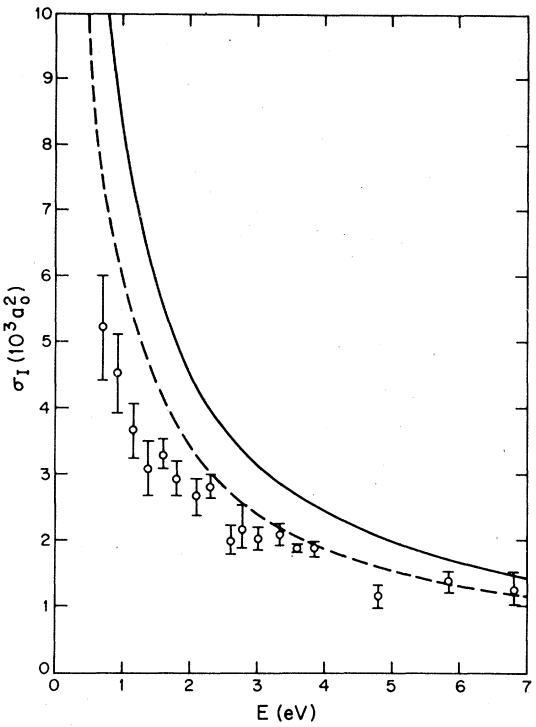

FIG. 1. Total integrated cross sections for 1.0-eV electrons on CsF. The experimental (Ref. 9) results (○) are for the most probable rotor state $\bar{j}=41$. The solid curve is the FBA result [Eq. (1.1)], and the dashed curve is the contribution to the latter from scattering with $\theta \leq 15°$.

All of the calculations listed in Table V were carried out in the complete representation. The general properties of the total integrated cross section discussed in Sec. II B are evident in these results. Once the calculation is taken beyond the FBA, the results are remarkably insensitive to the representation of the interaction potential or the scattering formalism used. This point will be reinforced by the results to be discussed in Sec. V B. The reason for this, of course, is that the major contribution comes from interactions at large distances where the dipole potential dominates and perturbation theory is applicable.

The arguments presented in Sec. II A with regard to the adiabatic approximation lead us to expect that the differences between the FBA result and more exact calculations should be quite insensitive to the initial rotor state. This is reflected in the results of the various perturbation-theoretic approaches. For example, the formula of Dickinson and Richards[26] can be cast in the form (for $D \geq 0.6$)

$$\Delta\sigma_I(\Delta j=\pm 1) = \frac{8\pi}{3}\frac{D^2}{k^2}\left(\ln D + 0.7535 + \frac{0.1437}{D^3}\right), \tag{5.1}$$

and the results of Mukherjee and Smith[23] can be approximated by the expression (for $D \gg 1.0$)

$$\Delta\sigma_I \simeq \frac{8\pi}{3}\frac{D^2}{k^2}(\ln D + 0.7673 - \eta), \tag{5.2}$$

where η accounts for transitions with $|\Delta j| \neq 1$ and is ~0.6 for $D \geq 2.0$. These two models were developed in the complete representation, but the results are independent of the initial rotor state. The agreement between (5.1) and (5.2) for the contribution for transitions with $|\Delta j| = 1$ is remarkable. The classical model of Dickinson,[31] developed in the FN representation, yields (for low energies)

$$\Delta\sigma_I = \frac{8\pi}{3}\frac{D^2}{k^2}\left(\ln D + 0.2224 \pm \frac{3\pi}{32D}\right), \tag{5.3}$$

where the sign of the last terms depends on whether (–) or not (+) the differential cross section in this model is constrained to be constant for $\theta \geq 60°$. We note the good agreement between (5.2) and (5.3) for large D, and the fact that (5.1)–(5.3) all agree in the logarithmic dependence on D.

The insensitivity to j is confirmed by the results of the close-coupling calculations presented in Table V, and is illustrated even more clearly in Table VI, where Nos. 1, 3, and 5 are taken from Table V. The difference between Nos. 3 and 5 in Table VI can be attributed to the slightly different value of the rotational constant B used by Allison. If Allison's value for the FBA cross section ($8424 a_0^2$) is used instead of No. 5 from Table V much better agreement with No. 3 results. The differences between Nos. 1 and 2 and between Nos. 3 and 4 can be attributed to incomplete convergence in the sum over final rotor states in the SF-frame calculations (we included $\Delta j \leq 4$). The results from the other two calculations in the FN representation (Nos. 6 and 7) are in remarkably good agreement with the close-coupling results.

We conclude that once $\Delta\sigma_I$ has been obtained in

TABLE VI. Correction to the FBA for the total integrated cross section for 1.0-eV electrons on CsF. Results of calculations for which the initial rotor state j is indicated were obtained in the complete representation, others were obtained in the FN representation.

No.	j	$\Delta\sigma_I$ (a_0^2)	Method	Reference
1	0	1237	CC [DCO(I)]	Present
2		1213	CC [DCO(I)]	Present
3	0	1246	CC [DCO(A)]	Present
4		1234	CC [DCO(A)]	Present
5	41	1151	CC	20
6		1221	EA	30
7		1393	CPT	31

TABLE VII. Partial integrated cross sections (in a_0^2) for 6.74-eV electrons on KI.

No.	σ_I ($j \to j'$) 0-0	0-1	0-2	0-3	Σ	Method
1		4412			4412	BI
2	107	3743	36	17	3903	BII
3	116	3734	69	21	3940	CC [DCO(R)]
4	158	3733	62	14	3967	CC [DCO(0.9)]
5	158	3729	65	15	3967	CC [DCO(1.35)]

the FN representation, or in the complete representation for one value of j, the total integrated cross section can be estimated quite accurately for *all* values of j, as long as $\delta \ll 1$. While we might expect a more exact treatment of the short-range potential than employed in any of these calculations to change the resulting corrections somewhat, there is no reason to believe that this essential conclusion would be affected.

We now consider the integrated cross section at the level of partial cross sections. Typical results are given in Table VII. All of the calculations were carried out in the complete representation. The hard-sphere cutoff of Rudge *et al.*[12] was chosen to yield an electron affinity corresponding to a reasonable estimate (0.7 eV). The other values of R_0 chosen yielded values of the electron affinity bracketing the estimated value, 0.85 and 0.35 eV for $R_0 = 0.9$ and $1.35a_0$, respectively. We see that while the total integrated cross section and that for $\Delta j = 1$ are quite insensitive to the model used, the partial cross sections for $\Delta j \neq 1$ show significant variation and that "tuning" to the electron affinity is not sufficient to determine unique results.

We can also use the results in Table VII and the scaling law for total integrated cross sections stated above to estimate the cross section for the most probable value of $\bar{j}$ (~75) for $T \sim 1000\,^\circ$K in the experimental measurements.[11,12] Using Nos. 1, and 4 or 5, we obtain a correction $\Delta\sigma_I = 445a_0^2$, which combined with the result of (1.3) for $j = 75$ yields $\sigma_I = 2623a_0^2$. This may be compared with the results of the distorted-wave calculation of Rudge *et al.*,[12] and the measurements of Slater *et al.*,[11] which are $2882a_0^2$ and $2010a_0^2$, respectively. We see that the former seems to be too large by about 10%, but more significantly to suggest a value of $\Delta\sigma_I$ lower by about a factor of 2. The differential and momentum-transfer cross sections from this calculation also seem too large, as we shall see. Regarding the measured cross section, it is almost certainly too small, since the FBA cross section (1.1) contributes about 1900 a_0^2 when integrated over only 2°.

TABLE VIII. Total momentum-transfer cross section for 1.0-eV electrons on CsF. Results of calculations for which the initial rotor state j is given were obtained in the complete representation, others were obtained in the ARM or FN representation.

No.	j	σ_M (a_0^2)	Method	Reference
1	0	1095	BI	
2	0	156	SPT	24
3	0	227	CC	21
4	0	317	CC [DCO(I)]	Present
5	0	331	CC [DCO(A)]	Present
6		323	CC [DCO(I)]	Present
7		335	CC [DCO(A)]	Present
8		168	Glauber	21
9		593	EA	21
10		357–418	EA	30
11		486	CPT	31
12	42	222	SPT	24
13	43	137	MFBA	25
14	41	368	CC	20
15	~41	90	Expt.	9

2. Momentum-transfer cross section

Illustrative results for the total momentum-transfer cross section are given in Table VIII. The FBA result No. 1 is not sensitive to j [see Eq. (2.6)]. In contrast to the total integrated cross section, the calculated results exhibit great sensitivity to the scattering formalism and potential approximation. Difficulties with the analysis of the experimental data discussed in the preceding and following sections also cast some doubt on the accuracy of the measured value. Thus the most that can be said is that the calculated and measured cross sections are, given the limitations of both, not completely inconsistent.

As stated in Sec. IIB, several of the methods used (Nos. 2, 8, 11–13) are not expected to be highly accurate for scattering at large angles, which make a significant contribution to the cross section. The difference between the results of the two adiabatic calculations Nos. 9 and 10 can probably be attributed to different approaches to the solution of the same equations. The larger difference between the close-coupling and adiabatic results Nos. 3 and 9 was taken, however, as evidence that[21] "the assumption of short collision-duration is not fully satisfied in this case"; and this seems to be supported by the comparison of Nos. 3 and 14 and by the semiclassical results Nos. 2 and 12, both of which exhibit considerable dependence on j.

The results Nos. 4–7 show that this interpretation is incorrect. The difference between Nos. 3 and 4 is primarily owing to contributions from transitions with $\Delta j = 3$ and 4 which contribute 29% of the

total in No. 4 and were not included in No. 3. The differences between Nos. 4 and 5 and between Nos. 6 and 7 are owing solely to the choice of cutoff for the dipole potential. A comparison of Nos. 5 and 14 is, then, a measure of the dependence on j in the complete representation, which we see is quite small and perhaps attributable to less-complete convergence in the extremely difficult calculations undertaken by Allison. Comparisons of Nos. 4 and 6, and Nos. 5 and 7, also support the validity of the adiabatic approximation since the remaining differences can most probably be attributed to contributions from transitions with $\Delta j > 4$. The use of different model potentials may be partially responsible for the differences between Nos. 4–7 and 9, and that between Nos. 2 and 12 is probably owing to the semiclassical approximations $j = \frac{1}{2}(j_i + j_f)$ and $j(j+1) \sim (j+\frac{1}{2})^2$ for the target angular momentum. The dependence of the cross section on j in these semiclassical calculations rapidly becomes weak as j increases.

Comparison with the results of Fabrikant[30] is particularly interesting. This model employed, in addition to the adiabatic approximation, an elegant application of R-matrix and effective-range theory. The range of results No. 10 corresponds to the limits obtained for *any* choice of the unknown energy-independent parameter representing the effect of all short-range (and nondipolar) forces. The fact that the present results Nos. 4–7 fall outside this range may only suggest that 1.0 eV is too high an energy for an effective-range approximation to be strictly valid.

Turning to a consideration of partial cross sections, we give typical results in Table IX. As expected, we see that partial momentum-transfer cross sections are even more model dependent than partial integrated cross sections. The total momentum-transfer cross section obtained in the distorted-wave calculation[12] for $j = 75$ is 234 a_0^2, as compared with No. 3 for $j = 0$; most of this difference must be attributable to the differences in collision formulation rather than to any breakdown of the adiabatic approximation. The good agreement of the distorted-wave result with No. 1 is therefore fortuitous and misleading. The measured value[11] for $\bar{j} = 75$ is 117a_0^2, again not inconsistent with the close-coupling results.

The general behavior of the total momentum-transfer cross section as a function of dipole moment is illustrated in Fig. 2. The BI, BII, and BIII cross sections were obtained in the FN representation and hence are rigorously independent of the initial rotor state of the molecule and proportional to E^{-1}. The curves plotted may be compared, therefore, with measurements or calculations for any molecule at any electron energy or temperature. Had the FBA cross sections been obtained in the complete representation they would differ negligibly, for small δ, from those shown. The range of results from close-coupling calculations for simple DCO model potentials for three alkali-metal halides are also shown. Those for LiF are for electron energies from 0.14 to 20 eV (see Sec. V B). Those for CsF are from Table VIII (Nos. 4–7, 14) for 1.0-eV electrons and from Ref. 20 for 2.0-eV electrons. Those for KI are from Table IX (Nos.

TABLE IX. Partial momentum-transfer cross sections (in a_0^2) for 6.74-eV electrons on KI.

No.	$\sigma_M(j \to j')$ 0-0	0-1	0-2	0-3	Σ	Method
1		307			307	BI
2	5	13	9	16	43	BII
3	6	10	19	16	51	CC [DCO(R)]
4	23	27	13	7	70	CC [DCO(0.9)]
5	16	19	17	9	61	CC [DCO(1.35)]

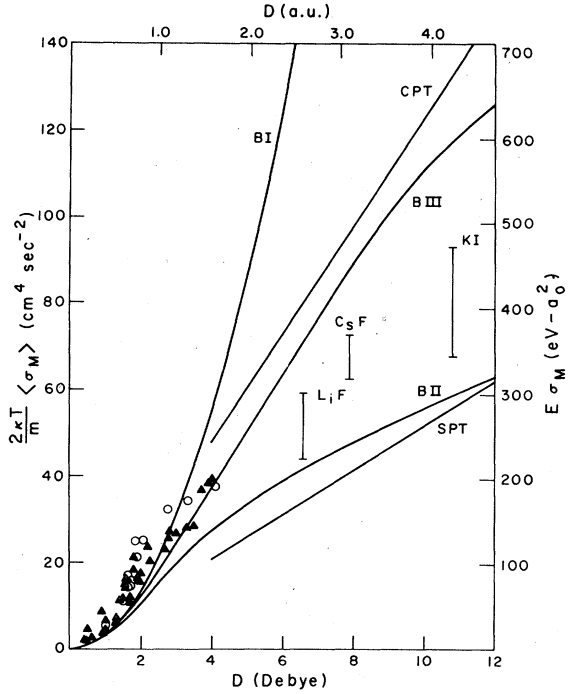

FIG. 2. Total momentum-transfer cross section as a function of dipole moment. The experimental data for $\langle\sigma_M\rangle$ are from thermal-energy swarm measurements: (▲) (Refs. 67 and 68) and (○) (Ref. 69). The calculated σ_M for LiF, CsF, and KI indicated by (I) are discussed in the text. The curves labeled BI, BII, and BIII are from the FBA in the FN representation, and may be referred to either ordinate. The curves labeled CPT and SPT were obtained using Eqs. (5.4) and (5.5), respectively.

3–5). We also show the result of the simple classical formula[31] for low energies

$$\sigma_M = \left(\frac{19\pi}{16}\right)\frac{\pi}{k^2}\left[D - \frac{3\pi}{152}\right], \tag{5.4}$$

and the result of the empirical fit to the semiclassical results[24] for $j \gg 1$ and $\delta \ll 1$

$$\sigma_M \simeq 1.55(\pi D/k^2) . \tag{5.5}$$

The total differential cross section in the classical model was constrained to go over to the FBA formula (1.4) for very small angles and to be constant for $\theta \geq 60°$. No such constraints were imposed in the semiclassical model and if they are removed in the classical model the term in [ ] in (5.4) vanishes, but more interestingly the term in ( ) in (5.4) becomes exactly $\frac{1}{2}\pi$. We have no reason to believe that the good agreement between these results and the BII curve is anything but fortuitous.

We also note that the BII and BIII results agree qualitatively with the flattening of the results from the swarm measurements for $D \geq 1$ a.u. and with the nearly linear dependence on D obtained from the semiclassical[24] and classical[31] models, and show that violation of unitarity is a significant consideration for larger dipole moments. Unitarization does not, however, improve the agreement with measurements for smaller dipole moments, in fact it makes it worse. The results of the model calculations fall between the BII and BIII results and are not inconsistent with the trend of the swarm data. In the absence of more accurate results for a particular molecule, a rough scaling based on the average of the BII and BIII curves appears most appropriate for large dipole moments.

3. *Differential cross section*

We expect differential cross sections, except for small angles, to be even more model dependent than momentum-transfer cross sections, and therefore do not expect more than qualitative agreement between the results of various calculations and measurements. As mentioned in Sec. II B there is, however, sharp qualitative disagreement between the results of calculations and measurements[8-12] which cannot be ignored.

The comparison of the results of some model calculations with one of the measurements,[11] shown in Fig. 3, addresses this issue. The essential feature of the model used to analyze the experimental data involved representation of the c.m. differential cross section as the FBA form (1.1) corrected by a three-term Legendre expansion, the coefficients of which were obtained in a least-squares fit to molecular-beam recoil data. The dotted curve in Fig. 3 is equivalent to a best fit, in a least-squares sense, of a three-term Legendre expansion to the same correction obtained from the DCO(1.35) model-potential calculation. Results obtained from calculations with the DCO(R) and DCO(0.9) model potentials display the same qualitative behavior. This is not surprising, if we consider the results in Tables V and VIII and recall that the total integrated and momentum-transfer cross sections are determined by the first one and two moments, respectively, of the Legendre expansion of the total differential cross section.

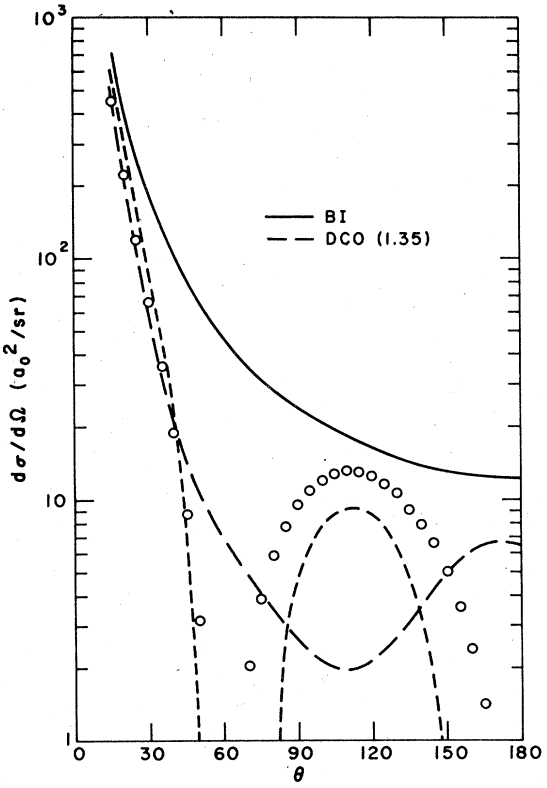

FIG. 3. Total differential cross section for 6.74-eV electrons on KI. The experimental (Ref. 11) results (○) are for most-probable rotor state $\bar{j}=75$. The dotted curve was obtained by taking only the first three moments in the Legendre expansion of the difference between the DCO (1.35) and BI results.

A plausible explanation for the sharp minima obtained from the measured data is, then, a lack of sensitivity in the analysis procedure to the higher moments of the c.m. differential cross section. This would also explain the much smaller disagreement (about a factor of 2) between the calculated and measured momentum-transfer cross sections than might be expected from comparison of the differential cross sections; and suggests

that it might be possible to extract accurate integrated and momentum-transfer (if not large-angle differential) cross sections from the measured data.

We also note the good agreement between the calculated and measured differential cross sections for $15° \leq \theta \leq 45°$, which is also obtained for the other two model potentials. For smaller angles the three model potentials yield cross sections which differ by less than 4%, again indicating insensitivity to the form of the potential at short range. The measured cross section, however, falls as much as 30% below the calculated value for $1° \leq \theta \leq 10°$. These angles are still very much larger than that ($\theta_0 \simeq 0.005°$) for which the cross section should have any significant dependence on the initial rotor state of the molecule. We conclude that the disagreement at small angles, which is reflected in the total integrated cross section as discussed above, is probably a spurious consequence of the particular model used to analyze the experimental data.

Reanalysis of the experimental data appears warranted and may be quite fruitful. All of the cross sections obtained here can be expressed analytically in the form

$$\frac{d\sigma}{d\Omega}(\theta) = \frac{d\sigma^{\mathrm{FBA}}}{d\Omega}(\theta) - \sum_{\lambda=0}^{26} \Delta A_\lambda P_\lambda(\cos\theta), \qquad (5.6)$$

where the first term is given by (1.1) and the ΔA_λ are known, and hence are ideally suited to such an analysis. We are led to suspect that the use of any of the DCO model-potential cross sections obtained here would yield a fit, in a least-squares sense, with the measured data that is no worse, if not significantly better, than that originally obtained, and are eager to see this hypothesis tested.

Total differential cross sections from the present DCO model-potential calculations are compared with the results of Rudge *et al.*[12] in Fig. 4. There is a significant difference between the results of close-coupling and distorted-wave calculations for the identical model potential, as noted above with regard to the total integrated and momentum-transfer cross sections. The large differences among the three close-coupling calculations at large angles emphasize the importance of an accurate treatment of the interaction potential at short range, which, of course, has not yet been done for KI. "Tuning" the exponential cut-off function (3.32) to the same electron affinity as used to define the hard-sphere cut-off function would presumably yield a result intermediate between the DCO(0.9) and DCO(1.35) curves, and hence an order of magnitude larger at 180° than the result obtained with the hard-sphere cut-off function. Since there is no reason to prefer one form of cut-off function to the other, tuning to the electron affinity may be a useful test, but it is certainly not a sufficient condition for the utility of a particular model potential, particularly for large-angle scattering.

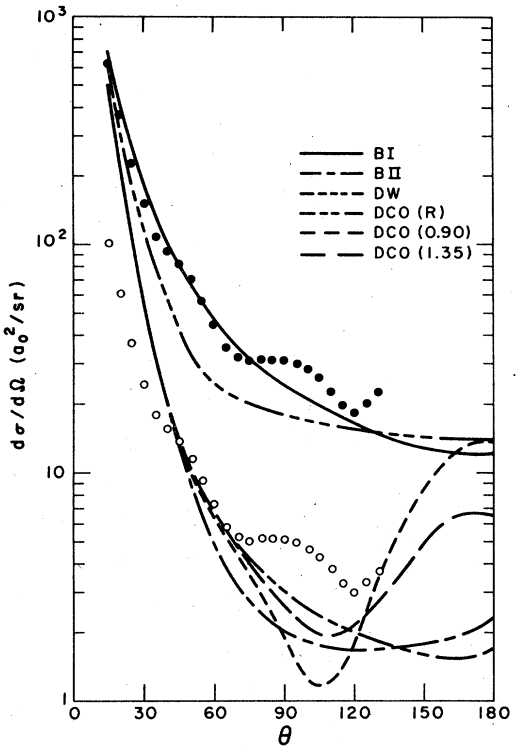

FIG. 4. Total differential cross section for 6.74-eV electrons on KI. The experimental data (Ref. 12) as originally normalized are indicated by (●) and as renormalized here by (○). The curve labeled DW is the result of the distorted-wave calculation (Ref. 12).

Finally, we note that with the original normalization of the relative experimental cross section to the results of calculations at 15° agreement with the FBA is obtained which is unique among measurements or calculations for the alkali-metal halides. We have taken the liberty of renormalizing (by a factor of 0.166) the experimental data to the results of the close-coupling calculations at 45°, where the excellent agreement among them indicates little sensitivity to the short-range interaction. The most plausible explanation for the remaining differences is greater experimental uncertainty at small angles and the weakness of the model potentials for large angles.

B. Results for LiF

One of the most interesting results obtained in the present study is a pair of shape resonances which occur for incident electron energies ~2.0 eV. These are discussed in detail in Sec. V B 1. In Secs. V B 2–V B 4 we discuss the integrated,

TABLE X. Total momentum-transfer cross section and $\Delta\sigma_I$ for the LiF DCO(0.5) potential calculated in the BF frame, and in the SF frame for $j=0$.

	σ_M (a_0^2)		$\Delta\sigma_I$ (a_0^2)	
E (eV)	BF	SF	BF	SF
0.544	512	508	1363	1504
2.0	121	121	376	391
3.0	84	84	252	258

momentum-transfer, and differential cross sections, paying particular attention to comparison between results obtained using various potential surfaces and collision approximations.

Since the adiabatic approximation was invoked in the most elaborate of these calculations, those with the SE and SEP surfaces, we have also done calculations for the DCO(0.5) potential completely in the BF (FN representation) and SF (complete representation) frames at three energies. The results are given in Table X, and suffice to demonstrate the validity of the adiabatic approximation since only the long-range dipole potential is at issue here. No differences are observed which cannot be attributed simply to numerical errors associated with convergence.

1. Resonances

The possible existence of a resonance or resonances in electron scattering from the alkali-metal halides was first suggested by Jordan and Luken[70] in a study of LiCl. The first evidence of such an effect appeared in the present SE calculations[14] for the LiF momentum-transfer cross section. In the following sections we will discuss the effect of these resonances on scattering cross sections, but in this section we find it more useful to discuss their properties from the point of view of molecular structure.

In view of the discussion of the adiabatic approximation in preceding sections we believe that calculations in the BF frame can provide an accurate description of the scattering process for low symmetries. Since the approximations involved in these calculations are essentially those involved in most conventional molecular-structure calculations, they should be particularly appropriate for resonances.[71]

One manifestation of resonances in scattering calculations is rapid variation in the eigenvalues of the scattering matrix, which can be conveniently studied by considering the sum of the eigenphases. These results for the SE(36) surface from the BF-frame calculations for the Σ and Π ($m_l=0$ and 1, respectively) symmetries are shown in Fig. 5. Notable features are the near coincidence of the two resonances in energy, but the significantly different widths. By studying the individual eigenphases we find that the Π resonance has a mixture of p- and d-wave character, and that the Σ resonance has a complicated s-p-d character. This is illustrated in Fig. 6 for the latter.

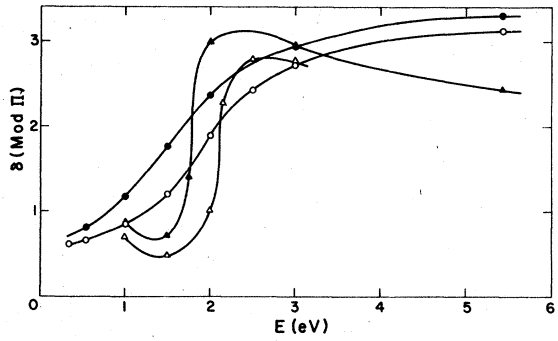

FIG. 5. Eigenphase sums for the LiF SE(○, △) and SEP(●, ▲) surfaces from calculations in the BF frame. The Σ and Π symmetry results are indicated by (△, ▲) and (○, ●), respectively.

In an earlier paper[14] we attributed the broad resonance feature in the momentum-transfer cross section entirely to the Π resonance, which was consistent with the prediction of Jordan and Luken[70] that a Σ resonance, if it existed, would occur at a much higher energy. Stimulated by the results of the subsequent self-consistent-field (SCF) calculations by Stevens[72] (to be discussed below), calculations with a much finer energy mesh than used earlier revealed the existence of the Σ resonance.

We should emphasize that these must be de-

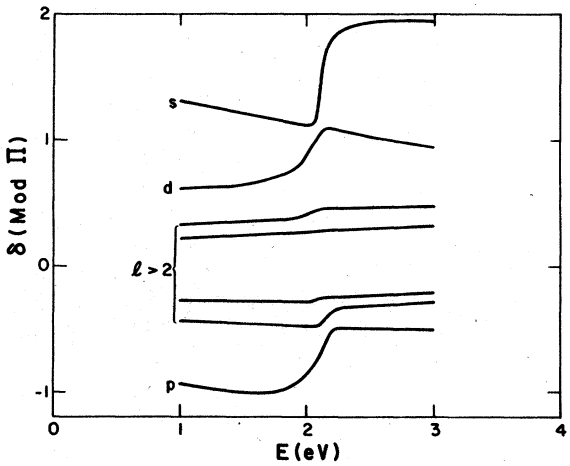

FIG. 6. Individual eigenphases for the LiF SE surface from the Σ-symmetry BF-frame calculation. The dominant angular momenta below the resonance region are indicated.

scribed as shape resonances since no closed channels were included in these calculations, and that they did not appear in calculations employing the static or any of the model-potential surfaces. Neither did they appear when the full exchange potential was combined with a truncated static potential, so it would be incorrect to attribute the resonances solely to exchange. The importance of the short-range potential was dramatically illustrated in test calculations in which the matching radius R_{max} was reduced from the value $200a_0$ usually used to $\sim 10a_0$, without destroying the resonant character of the eigenphase sum. Quantitative change was, of course, observed.

The calculations of Stevens[72] employed a procedure similar to that of Krauss and Mies[73] to generate potential-energy curves for the resonance states as a function of internuclear separation. The results show that both resonances correlate with the system $Li(2\,^2P) + F^-(1\,^1S)$ in the separated-atom limit. At the approximate minima ($\sim 3.0a_0$) of the resonance curves and that for the ground state of LiF, the Σ and Π resonances are ~1.8 and ~1.5 eV, respectively, above the ground state. Plots of the amplitude of the valence-electron component of the total wave function qualitatively agree with the angular momentum character of the resonances described above.

In order to test the sensitivity of the resonance positions to polarization we have also performed calculations with the SEP(36) surface. This also provides a more consistent comparison with the SCF results, since polarization is taken into account in the latter. The calculations were performed for a range of R_c in (3.29) from $2.5a_0$ to $3.5a_0$, thereby spanning a physically reasonable range. The positions of the resonances shifted to lower energies by ~0.5 eV at most. The choice $R_c = 3.0a_0$ reduces the energy of the Σ resonance ~0.3 eV and that of the Π resonance ~0.4, resulting in quite good agreement with the results of Stevens. These results are also shown in Fig. 5.

The relatively small effect of polarization compared with that obtained for other molecules[74] can be understood by comparing the relative strengths of the dipole and spherical (α_0) adiabatic polarization potentials. Expressed simply in terms of their asymptotic forms, the two are comparable for $R \sim 1.0a_0$, but the former is an order of magnitude larger for $R \sim 3.0a_0$ and two orders of magnitude larger for $R \sim 9.0a_0$. For nonpolar molecules, on the other hand, the polarization and quadrupole potentials may be quite comparable over the analogous range of R.

In order to see if these resonances are indeed a general property of the alkali-metal halides we have performed calculations in the BF frame using the S and SE surfaces for LiCl, NaF, and NaCl. The eigenphase sums for the Σ and Π symmetries were calculated over the range of electron energies 0.25–5.0 eV. Preliminary results indicate resonances in both symmetries for NaF and NaCl at about 3.2 and 0.9 eV, respectively. The resonance widths are comparable to the widths for the LiF resonances. Neither system exhibited any resonant character with the S surface.

To our great surprise, no resonance was found in either symmetry for LiCl at the equilibrium distance ($\sim 3.8a_0$). We cannot, of course, exclude the possibility that the resonances are very much narrower for LiCl than for the others and went undetected with our energy mesh (0.25 eV), or lie outside the energy range studied to date. Some evidence for the existence of a resonance or resonances for LiCl was obtained in calculations for a larger internuclear separation ($\sim 4.5a_0$), which indicated resonant behavior in the π symmetry at ~0.5 eV above the neutral potential.

While preliminary, these results strongly suggest that resonances may be not at all uncommon in electron scattering by strongly polar systems,[75] and that such features may substantially influence momentum-transfer and differential cross sections. Since the present results for the resonance energies do not correlate in any obvious way with simple properties of these molecules (e.g., D, α_0, I_P, the electron affinity, or equilibrium molecular internuclear separation), it is not possible at this point to generalize to the other alkali-metal halides or to other interesting related systems such as the alkali-metal hydroxides.

2. *Integrated cross section*

Partial and total integrated cross sections from calculations in the complete representation at three representative energies below (0.544 eV), near (2.0 eV) and above (3.0 eV) the resonance region are given in Table XI. Trends illustrated by these results hold over the entire energy range (0.14–20.0 eV) studied. We see that the S(36) and simpler models of the static surface used in the close-coupling calculations yield total integrated cross sections within 2% of the SE(36) result. The unitarized Born (BII) results are accurate to better than 4%, and even the BI results are in error by no more than 15%. These same observations hold for the partial cross sections for the transition $\Delta j = 1$.

The partial cross sections for other transitions are not given nearly as well by the simpler models. These transitions are only indirectly coupled by the dipole potential and hence are much more sensitive to the short-range component of the po-

TABLE XI. Partial and total integrated cross sections (in a_0^2) for LiF.

E (eV)	Model	σ_I ($j \to j'$) 0-0	0-1	0-2	0-3	0-4	Σ
0.544	SE(36)	776.2	9791.2	258.4	77.3	19.7	10942.8
	S(36)	737.0	9788.3	270.4	96.4	21.4	10913.5
	S(11)	725.6	9797.0	269.8	84.7	17.9	10895.0
	S(2)	711.9	9769.1	304.0	92.3	19.1	10896.4
	DCO(0.5)	758.1	9705.5	269.1	83.0	20.6	10836.3
	BII	447.7	9988.1	183.9	65.5		10685.2
	BI		12340.2				12340.2
2.0	SE(36)	246.3	3177.7	73.4	9.9	7.1	3514.4
	S(36)	181.3	3160.5	84.6	29.0	5.2	3460.6
	S(11)	157.4	3207.7	79.9	15.2	2.2	3462.4
	S(2)	211.5	3199.0	68.6	15.3	3.9	3498.3
	DCO(0.5)	186.9	3160.9	84.1	25.3	5.6	3462.8
	BII	121.7	3214.7	49.9	17.8		3404.1
	BI		3854.1				3854.1
3.0	SE(36)	126.1	2237.7	56.8	10.6	2.7	2433.9
	S(36)	112.7	2220.7	54.6	14.5	3.1	2405.6
	S(2)	155.5	2223.7	44.8	10.9		2434.9
	DCO(0.5)	122.4	2217.5	55.9	15.5	3.4	2414.7
	BII	81.3	2245.6	33.3	11.9		2372.1
	BI		2672.4				2672.4

tential surface. We note in particular the results for the S(11) and S(36) surfaces at the two lowest energies. Preliminary results obtained for $\lambda_{max} \sim 11$ indicated that convergence had been reached at this level. Further study revealed that this was a false "plateau" and that many more moments were required in the expansion (3.20) in order to completely account for the nuclear singularity at the Li nucleus which is much further from the c.m. than the F nucleus.

Results for $\Delta\sigma_I$ are presented in Table XII. Differences between these results and those of calculations carried out in the SF frame for the SE(36) surface, some of which are given in Table XI, never exceed the expected numerical accuracy of either. Based on the previous results and discussion we conclude that the results presented in Table XII can be used with confidence to generate the total integrated cross section to an accuracy of better than 1% for any initial rotor state for which $\delta \ll 1$.

TABLE XII. Correction to the FBA for the total integrated cross section for LiF for the SE(36) surface in the BF frame.

E (eV)	$E\Delta\sigma_I$ (eV a_0^2)	E (eV)	$E\Delta\sigma_I$ (eV a_0^2)
0.136	769.4	2.50	700.3
0.340	745.4	3.00	710.8
0.544	712.4	4.00	710.4
1.00	717.7	5.44	699.3
1.50	649.3	7.00	685.2
1.75	616.8	10.00	664.7
2.00	662.5	20.00	596.0

Since the resonances are a property of the short-range potential, there is little or no observable effect in the total integrated cross section which is dominated by high, nonpenetrating, partial waves. A resonance feature is nicely revealed, however, in the results in Table XII, since this quantity is a measure of the interaction at short range. It is also obvious that the effect of the resonances would be more pronounced in partial cross sections for transitions with $|\Delta j| \neq 1$ than for those with $|\Delta j| = 1$. In spite of the extremely small rotational spacings involved, such measurements can be contemplated. Preliminary results of experiments using magnetic selection to detect individual rotational transitions with $|\Delta j| = 1$ have already been reported.[76]

We note that $E\Delta\sigma_I$ is slowly varying and very nearly linear in E above the resonance region. The insensitivity of $E\Delta\sigma_I$ to E was noted in, or can be inferred from the results of, earlier model studies[23,25,26,30,31] which treated only the dipole potential, and is also evident in the present BII results, given in Table XI, which are 901 eV a_0^2. In the FN representation the BII and BIII results are 915 and 691 eV a_0^2, respectively. The difference between the two BII results is owing to convergence. For comparison the semiclassical[23] and classical[31] models (5.2) and (5.3) yield 852 and 894 ∓ 87 eV a_0^2, respectively. Using (5.1) or (5.2) for transitions with $|\Delta j| = 1$ only we obtain 1305

TABLE XIII. Partial and total momentum-transfer cross sections (in a_0^2) for LiF.

		$\sigma_M(j \to j')$					
E (eV)	Model	0-0	0-1	0-2	0-3	0-4	Σ
0.544	SE(36)	171.5	199.2	83.6	78.9	27.3	560.5
	S(36)	123.3	178.1	96.7	107.0	30.3	535.4
	S(11)	120.9	163.8	101.1	88.0		473.8
	S(2)	118.3	90.0	124.5	95.6		428.4
	DCO(0.5)	137.5	170.7	87.9	83.4	28.2	507.7
	BII	47.7	142.5	114.9	82.0		387.1
	BI		1400.6				1400.6
2.0	SE(36)	78.8	84.7	27.9	8.8	6.5	206.7
	S(36)	32.3	25.1	38.7	25.7	7.4	129.2
	S(11)	26.5	34.1	35.6	14.6		113.8
	S(2)	63.4	58.3	22.0	13.4		157.1
	DCO(0.5)	28.5	27.1	31.8	25.9	7.6	120.9
	BII	13.0	39.1	31.0	22.2		105.3
	BI		381.1				381.1
3.0	SE(36)	24.5	31.7	25.0	11.5	3.7	96.4
	S(36)	22.9	24.1	24.7	15.9	4.3	91.9
	S(2)	43.5	42.9	13.8	10.7		110.9
	DCO(0.5)	23.2	19.5	20.9	15.3	4.6	83.5
	BII	8.7	25.8	20.7	14.8		70.0
	BI		254.1				254.1

and 1309 eV a_0^2, respectively, in excellent agreement with the results given in Table XI.

3. Momentum-transfer cross section

Representative results for partial and total momentum-transfer cross sections are given in Table XIII. Sensitivity to the form of the short-range interaction is clearly much greater than for the integrated cross sections. Compared with the results of the close-coupling calculations, the BI results are now poor for the transition with $\Delta j = 1$. The BII results are qualitatively correct, however, and suggest that violation of unitarity rather than inaccurate treatment of the short-range interaction is the major flaw in the simple formula (1.2).

It is interesting to note that the DCO(0.5) results are generally in better agreement with the S(36) results than are either the S(2) or S(11) results. This is somewhat misleading, as can be seen from the results shown in Fig. 7. No one of the DCO model potentials yields uniformly better agreement than the others over this energy range, but all seem to lie within a general envelope with relatively constant upper and lower limits. The S(2) and S(11) results also lie within or near this envelope. This behavior is in general qualitative accord with that predicted by the effective-range approach of Fabrikant,[30] the stated condition for the validity of which yields $E \ll 6$ eV for LiF. The momentum-transfer cross section for highly polar molecules from this model can be expressed as[69]

$$\sigma_M = (\pi/k^2)[\alpha + \beta \sin(\gamma + \mu \ln k^2)], \tag{5.7}$$

where α, β, and μ are constants depending only on the dipole moment D, and γ depends on both D

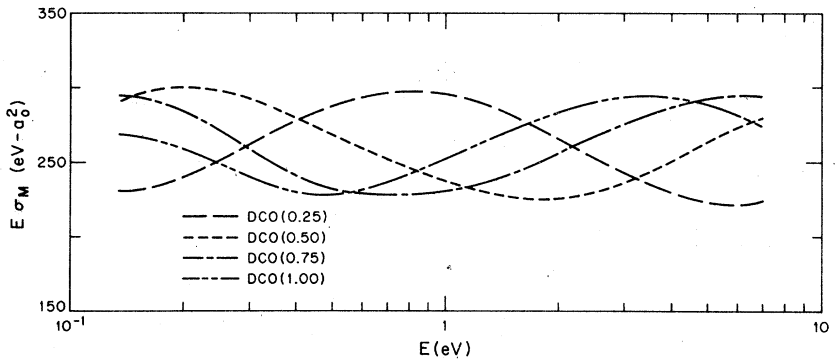

FIG. 7. Total momentum-transfer cross section for LiF for several DCO model potentials.

and all short-range (and nondipolar) interactions.

The values of α, β, and μ have not been given for LiF, but can be roughly estimated from values given for other molecules.[30,69] We estimate $\alpha \simeq 7.3$, $\beta \simeq 0.60$, and the period $T(=2\pi/\mu) \simeq 4.3$ for LiF. In comparison the present DCO results in Fig. 7 have $\alpha \simeq 6.1$, $\beta \simeq 0.80$, and $T \simeq 3.7$. The agreement is reasonably good, but it must be noted that at the lowest energies the stated condition for the validity of the effective-range approximation is well satisfied. The differences may be attributable to the approximations made in the derivation of (5.7), or to our estimates of α, β, and μ.

This simple picture breaks down in the resonance region, where the SE results differ dramatically from the others, particularly for the transitions with $\Delta j = 0$ and 1. The peak of the resonance lies well outside the upper limit of the envelope of the present DCO results, or that based on (5.7). An effective-range approach is probably inadequate for this type of resonance.

Results for the total momentum-transfer cross section are presented in Table XIV. These results, again obtained from calculations carried out completely in the BF frame, are in excellent agreement with the results of calculations carried out in the SF frame for the SE(36) surface, some of which are given in Table XIII. As for the results in Table XII, we believe that these results are valid for any initial rotor state for which $\delta \ll 1$.

The effect of the resonance is more clearly seen in Fig. 8, as an increase of almost a factor of 2 in $E\sigma_M$ at ~1.8 eV. Comparing the various results away from the resonance region we note several trends. The BII and BIII results span the results of the more accurate calculations. The semiclassical[24] and Glauber[77] results are practically indistinguishable and too small, a consequence of the large underestimate of the differential cross section at large angles. The classical[31] results are, on the other hand, too large, a consequence of the fact that the differential cross section was taken to be constant for $\theta \geq 60°$. The rapid change in the classical result around 10.0 eV is owing to the additional condition imposed that the differential cross section is not smaller than the corresponding hard-sphere cross section $\frac{1}{4}R_e^2$ at the given energy, where R_e is taken to be the equilibrium internuclear separation.

The rapid rise in the SE results above 5.0 eV is an interesting effect, especially when it is noted that the momentum-transfer cross sections obtained from the experimental measurements of Stern and co-workers[10,11] also displayed similar behavior. Consideration of the partial cross sections revealed a sharply increased relative contribution from transitions with $\Delta j > 2$ in the SF-frame results. This behavior was also seen in calculations with the S(36) and S(2) surfaces but not with the DCO model potentials. It is apparently the consequence of greater penetration of partial waves with finite angular momenta into the short-range region, where they can be strongly mixed by the interaction. Simple models of the interaction clearly become poor at higher energies.

TABLE XIV. Total momentum-transfer cross section for LiF for the SE(36) surface in the BF frame.

E (eV)	σ_M (a_0^2)	E (eV)	σ_M (a_0^2)
0.136	2060.6	2.50	130.9
0.340	917.4	3.00	95.43
0.544	560.2	4.00	65.60
1.00	284.8	5.44	49.98
1.50	243.1	7.00	42.41
1.75	246.6	10.00	34.61
2.00	205.9	20.00	23.68

We note finally that the inclusion of the estimated adiabatic polarization potential had negligible effect on the momentum-transfer cross section, except to the extent it shifted the resonance position.

4. Differential cross section

The total differential cross sections for the SE(36), S(36), DCO(0.5) surfaces, and from the FBA formula (1.1) at 0.544, 2.0, and 3.0 eV are

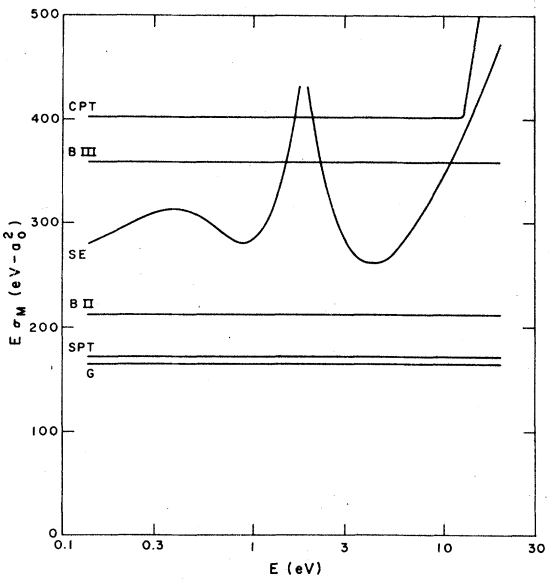

FIG. 8. Total momentum-transfer cross section for LiF. The curves labeled CPT and SPT were obtained using Eqs. (5.4) and (5.5), respectively, and that labeled G is the result of Glauber calculations (Ref. 77).

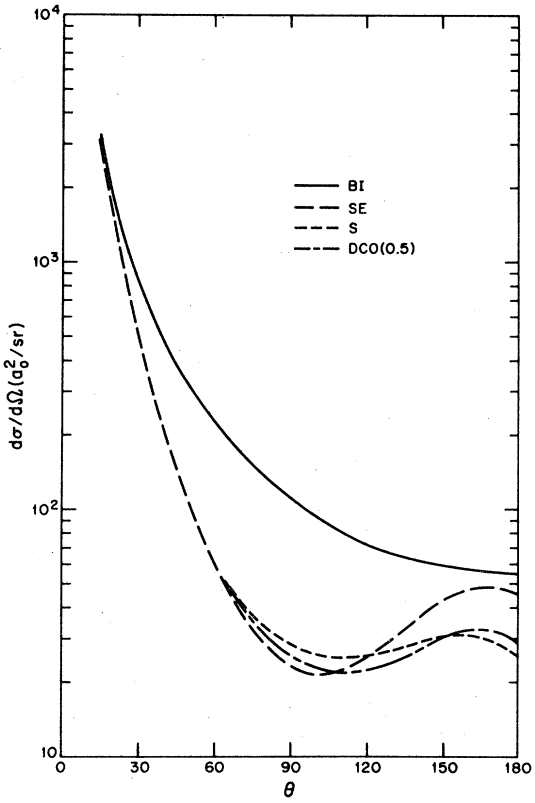

FIG. 9. Total differential cross section for 0.544-eV electrons on LiF.

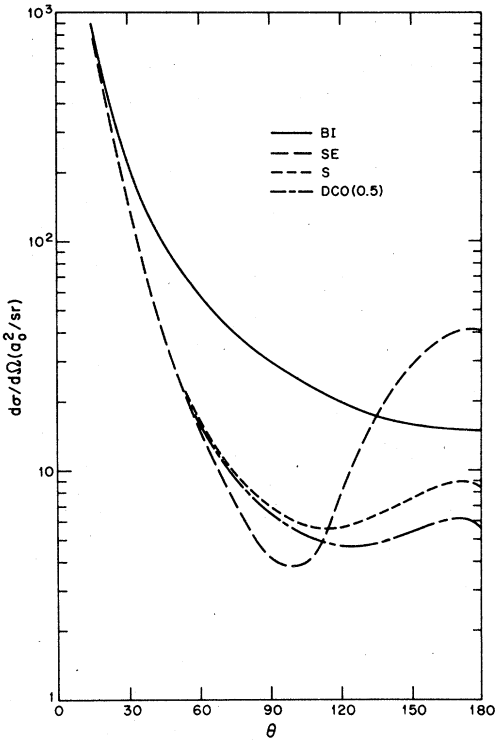

FIG. 10. Total differential cross section for 2.0-eV electrons on LiF.

presented in Figs. 9, 10, and 11, respectively. These results serve to illustrate several general features. At small angles ($\theta \lesssim 15°$) the various models are all within 10% of the FBA result and within 4% of each other, and there is little sensitivity to the model for angles $\lesssim 60°$. At larger angles much greater sensitivity to the interaction at short range is noted. While the total momentum-transfer cross sections for the SE, S and DCO surfaces differ by not more than 25% (excepting the resonance region), much larger differences are observed in the total differential cross sections. As for the momentum-transfer cross sections, the DCO(0.5) results for differential cross sections were in best overall accord with the results from the S surface. Similarly, the results for other DCO model surfaces differ for large angles by much more than the corresponding total momentum-transfer cross sections.

The 2.0-eV results illustrate behavior in the resonance region. The differential cross section for the SE surface is significantly different from the other models considered, being characterized by a deep minimum at ~100° and a pronounced rise at large angles. The enhanced region of backscattering primarily affects the transitions $\Delta j = 0$

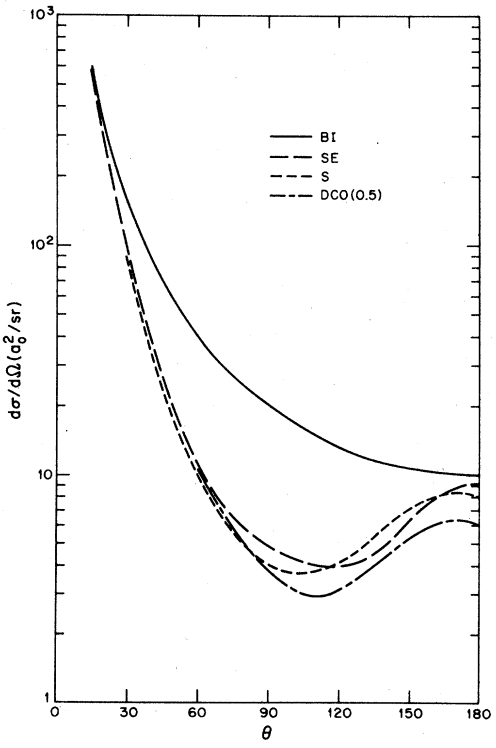

FIG. 11. Total differential cross section for 3.0-eV electrons on LiF.

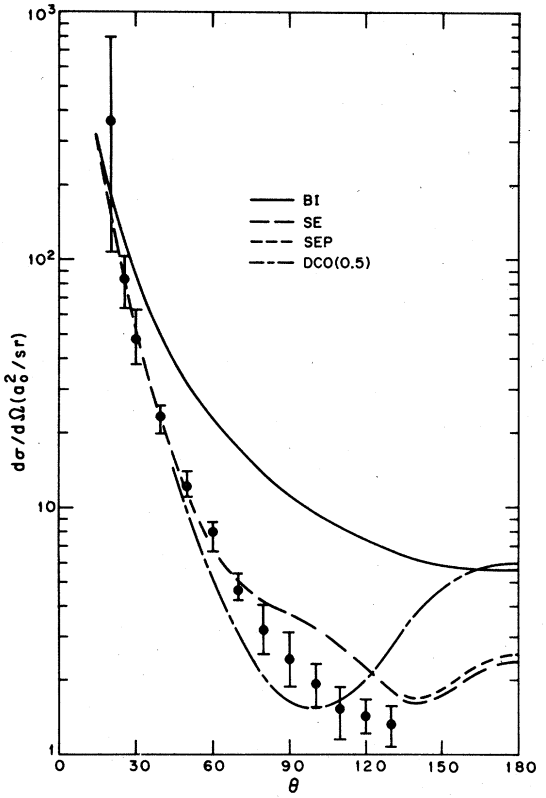

FIG. 12. Total differential cross section for 5.44-eV electrons on LiF. The experimental results (Ref. 13) (Φ) have been normalized to the present results at 40°.

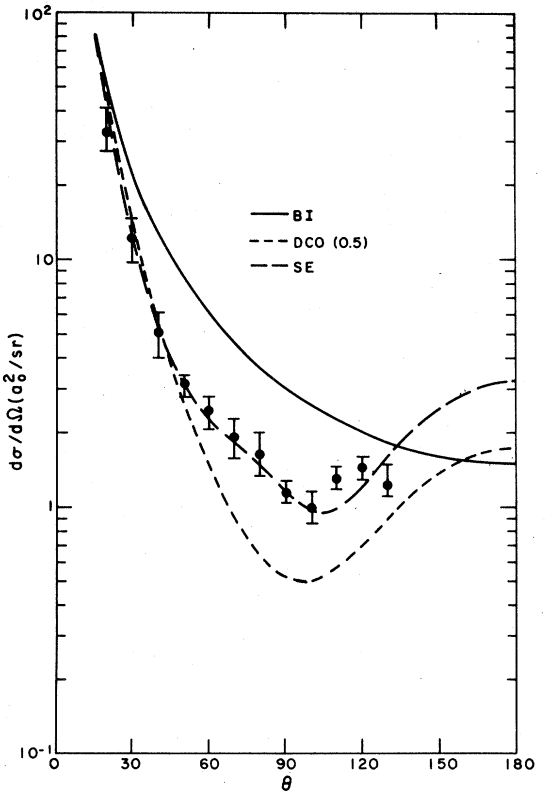

FIG. 13. Total differential cross section for 20.0-eV electrons on LiF. The experimental results (Ref. 13) (Φ) have been normalized to the present results at 40°.

and 1 and is owing to the electron effectively being trapped by the potential barrier, and therefore having greater time to experience the short-range part of the potential that most influences high-angle collisions. In a plot of the differential cross sections as a function of energy the resonance region is characterized by a pronounced minimum at ~100° and a maximum for angles ≳135°.

In Figs. 12 and 13, we compare the total differential cross section for the various models at 5.44 and 20.0 eV with the relative experimental measurements of Vušković *et al.*[13] In spite of the fact that the calculations were all carried out in the SF frame for the ground rotor state and the measurements involved molecules with $\bar{j} \sim 16$, we believe on the basis of earlier discussion that they can be quantitatively compared. We have normalized their results to our SE cross section at 40°. The agreement is quite encouraging, especially when it is noted that only the SE cross section has a shape reasonably resembling that of the experimental results.

The discrepancy in the 5.44-eV results at large angles may be owing to our approximate treatment of exchange, but there are also systematic experimental uncertainties, e.g., vibrational excitation and scattering by dimers, which could affect the results. The results at 20.0 eV show clearly that the sharp increase in the total momentum-transfer cross section at the higher energies is associated with increased backward scattering. The 5.4-eV results also illustrate the quite small effect of polarization.

Differential cross sections obtained from the classical model[31] and from Glauber calculations[77] for LiF are in quite good agreement with the present results for small angles. Differences are typically 20% and 10%, respectively, at 45° and decrease at smaller angles. The classical model predicts an angular dependence of $\sin^{-3\frac{1}{2}}\theta$, whereas the Glauber model yields $\sin^{-2\frac{1}{2}}\theta$. The classical model is in much better agreement with the present results in shape for $15° \lesssim \theta \lesssim 45°$, but it must be noted that the Glauber results are generally in better agreement in magnitude.

VI. SUMMARY AND CONCLUSIONS

The primary objective of this work has been an extensive set of cross sections for electron scattering by LiF that is considerably more accurate than available heretofore for any highly polar

molecule. Close-coupling calculations were performed employing the full static potential plus a local energy-dependent model-exchange potential. The effect of polarization was also investigated. The results have been used as a standard of comparison for calculations employing simpler models of the interaction potential and/or other approximations to the solution of the scattering problem. We have investigated some simpler models, specifically close-coupling calculations using only the static potential (and limited approximations thereto) and cut-off dipole model potentials, and calculations employing unitarized Born formulations. Comparisons were also made with results of others who used semiclassical, classical, effective-range, and Glauber approximations in calculations for the dominant dipole potential.

We can summarize the results of these comparisons as follows. Almost any approach that goes beyond the FBA will yield quite good results for the total or $\Delta j = \pm 1$ integrated cross section, and results for the total momentum-transfer cross section that are correct to within about 50%. The total differential cross section can be obtained quite accurately using the FBA for angles $\lesssim 15°$, and using rather simple approximations for angles $\lesssim 45°$. But for angles $\gtrsim 60°$ simple approximations can yield results that are seriously in error. The use of a cut-off dipole potential in close-coupling calculations appears to yield results for the total momentum-transfer cross section that are correct to within ~25%, but results for the large-angle differential cross section that are reliable only to within a factor of 2 or 3. Finally, partial cross sections, especially for transitions with $|\Delta j| \neq 1$, in each case exhibit greater sensitivity to the potential surface and scattering formalism than does the total cross section. Polarization was found to be a relatively unimportant effect.

A pronounced resonance feature was found in the static-model exchange results which is identified with shape resonances in both the Σ and Π body-frame symmetries. Similar features were found in NaF and NaCl but not in LiCl. These resonances can have a large effect on differential and momentum-transfer cross sections and it is not likely that they can be predicted or even reproduced except in fairly sophisticated calculations.

The static-model exchange calculations involved an alternative form of the frame-transformation approach, and thus a limited appeal to the adiabatic (fixed-nuclei) approximation. A secondary objective of this work has been, therefore, to test the validity of this approximation with several model studies. We conclude that, except for scattering near rotational thresholds, the total differential cross section for scattering out of the forward direction and the total momentum-transfer cross section can be reliably generated from body-frame $\underline{T}$-matrix elements calculated in the adiabatic fixed-nuclei approximation. The total integrated cross section and differential cross section for forward scattering can be calculated by correcting the SF frame FBA cross sections using BF-frame $\underline{T}$-matrix elements. This is of particular significance when comparing the results of calculations and measurements, since the BF-frame scattering quantities are independent of initial rotor state. In addition, it should be possible to obtain accurate SF-frame cross sections for any given rotor level by a simple algebraic transformation of the $\underline{T}$ matrices from a single BF-frame calculation.

Several points deserve further study. The present calculations are based on a local model-exchange potential, and while there is supporting evidence for the resonance features in LiF from the calculations of Stevens[72] and for the calculated differential cross sections from the measurements of Vušković *et al.*,[13] comparison with results of calculations involving exact treatment of exchange would be very useful. Calculations to this end are in progress. While the validity of the adiabatic approximation has been demonstrated and used here in a particularly favorable energy range, its usefulness at lower energies and near thresholds should be explored. Nevertheless, the present results are sufficiently encouraging that further calculations for several other polar molecules (LiH, HCN, and KOH) are now in progress. The simplifications introduced by the model exchange potential and the BF-frame formulation of the scattering equations also bring accurate close-coupling calculations for more complicated nonlinear polyatomic molecules, e.g., H_2O, into the realm of feasibility, and should also greatly facilitate calculations of vibrational-rotational excitation in polar molecules.

Note added in proof. The results of specific calculations of the parameters α, β, and T, for LiF, discussed in Sec. V B 3 using the ERT are 6.49, 0.80, and 4.20, respectively (I. I. Fabrikant, private communication).

ACKNOWLEDGMENTS

This work was supported in part by the U.S. National Science Foundation (RANN and Division of Engineering) and by the U.S. Department of Energy (Office of Basic Energy Sciences). One of us (L.A.C.) wishes to thank the members of Group T12 of the Los Alamos Scientific Laboratory for their kind hospitality and assistance during his tenure (1975–1977)

as a Visiting Staff Member and for providing computer time for a portion of the calculations. We would like to thank Dr. W. Stevens for providing us with preliminary results of his structure calculations on LiF and LiF ; Dr. S. Trajmar for sending us the results of his measurements on LiF in advance of publication; and Dr. A. Allison, Dr. Y. Itikawa, and Dr. I. Shimamura for kindly providing us with additional details and results of their calculations. We also thank Dr. G. B. Schmid for performing additional complementary calculations which have helped to complete several of the tables. Finally, we gratefully acknowledge useful discussions with Dr. N. F. Lane, Dr. M. A. Morrison, Dr. W. P. Reinhardt, and Dr. R. C. Stern on the general aspects of this project and thank the former two for helpful comments and suggestions on the early drafts of the manuscript.

---

*Present address: Group T4, MS/212, Los Alamos Scientific Laboratory, Los Alamos, N. M. 87545.
†Staff Member, Quantum Physics Division, National Bureau of Standards, Boulder, Colo. 80309.

[1]H. S. W. Massey, Proc. Cambridge Philos. Soc. 28, 99 (1932).
[2]O. H. Crawford, A. Dalgarno, and P. B. Hayes, Mol. Phys. 13, 181 (1967).
[3]K. Takayanagi, J. Phys. Soc. Jpn. 21, 507 (1966).
[4]S. Altshuler, Phys. Rev. 107, 114 (1957).
[5]See the review by K. Takayanagi and Y. Itikawa [Adv. At. Mol. Phys. 6, 105 (1970)]; and also Ref. 7. A new review has been prepared by Y. Itikawa, Phys. Rep. (to be published).
[6]W. R. Garrett, Phys. Rev. A 11, 509 (1975).
[7]W. R. Garrett, Mol. Phys. 24, 465 (1972).
[8]R. C. Slater, M. G. Fickes, and R. C. Stern, Phys. Rev. Lett. 29, 333 (1972).
[9]R. C. Slater, M. G. Fickes, W. G. Becker, and R. C. Stern, J. Chem. Phys. 60, 4697 (1974).
[10]W. G. Becker, M. G. Fickes, R. C. Slater, and R. C. Stern, J. Chem. Phys. 61, 2283 (1974).
[11]R. C. Slater, M. G. Fickes, W. G. Becker, and R. C. Stern, J. Chem. Phys. 61, 2290 (1974).
[12]M. R. H. Rudge, S. Trajmar, and W. Williams, Phys. Rev. A 13, 2074 (1976).
[13]L. Vuškovíc, S. K. Srivastava, and S. Trajmar, J. Phys. B (to be published).
[14]Preliminary results of these calculations have been reported: L. A. Collins and D. W. Norcross, Phys. Rev. Lett. 38, 1208 (1977).
[15]M. J. Seaton, Proc. Phys. Soc. 77, 174 (1961).
[16]P. M. Chase, Phys. Rev. 104, 838 (1956).
[17]K. Takayanagi, Prog. Theor. Phys. Suppl. 40, 216 (1967). This result was obtained by considering the *exact* expression for the scattering amplitude, in the context of the adiabatic approximation. See E. S. Chang and A. Temkin, Phys. Rev. Lett. 23, 399 (1979), and references therein, for further discussion for special cases.
[18]W. R. Garrett, Phys. Rev. A 4, 2229 (1971).
[19]See Refs. 26 and 31, and references therein.
[20]A. C. Allison, J. Phys. B 8, 325 (1975).
[21]Y. Itikawa, J. Phys. Soc. Jpn. 41, 619 (1976).
[22]Y. Itakawa, J. Phys. Soc. Jpn. 42, 1334 (1977).
[23]D. Mukherjee and F. T. Smith, Phys. Rev. A 17, 954 (1978).
[24]A. P. Hickman and F. T. Smith, Phys. Rev. A 17, 968 (1978).
[25]M. R. H. Rudge, J. Phys. B 7, 1323 (1974).
[26]A. S. Dickinson and D. Richards, J. Phys. B 8, 2846 (1975).
[27]K. Takayanagi, Prog. Theor. Phys. 52, 337 (1974).
[28]O. Ashihara, I. Shimamura, and K. Takayanagi, J. Phys. Soc. Jpn. 38, 1732 (1975).
[29]K. Onda, J. Phys. Soc. Jpn. 40, 1437 (1976).
[30]I. I. Fabrikant, Sov. Phys.-JETP 44, 77 (1976).
[31]A. S. Dickinson, J. Phys. B 10, 967 (1977).
[32]M. E. Rose, *Elementary Theory of Angular Momentum* (Wiley, New York, 1957).
[33]A. M. Arthurs and A. Dalgarno, Proc. R. Soc. A 256, 540 (1960).
[34]E. S. Chang and U. Fano, Phys. Rev. A 6, 173 (1970).
[35]S. Hara, J. Phys. Soc. Jpn. 22, 710 (1967).
[36]A. Temkin and K. V. Vasavada, Phys. Rev. 160, 109 (1967)
[37]W. R. Garrett, Phys. Rev. A 11, 1297 (1975).
[38]P. G. Burke and A.-L. Sinfailam, J. Phys. B 3, 641 (1970).
[39]Y. Itikawa, J. Phys. Soc. Jpn. 27, 444 (1969).
[40]N. Chandra, Phys. Rev. A 12, 2342 (1975).
[41]A detailed examination of the limits of validity of the FBA has been provided by C. W. Clark [Phys. Rev. A 16, 1419 (1977)].
[42]M. J. Seaton, Proc. Phys. Soc. 89, 469 (1966).
[43]R. D. Levine, J. Phys. B 2, 839 (1969).
[44]R. D. Levine, Mol. Phys. 22, 497 (1971).
[45]N. Chandra, Phys. Rev. A 16, 80 (1977).
[46]M. A. Morrison and L. A. Collins, Phys. Rev. A 17, 918 (1978).
[47]See Eq. (44) in Ref. 35 and Eq. (15) in Ref. 38.
[48]The procedures used are described in detail by L. A. Collins [Ph.D. thesis (Rice University, 1975) (unpublished)] and by M. A. Morrison [Ph.D. thesis (Rice University, 1976) (unpublished)].
[49]M. A. Morrison, N. F. Lane, and L. A. Collins, Phys. Rev. A 15, 2186 (1977).
[50]H. S. W. Massey and R. O. Ridley, Proc. R. Soc. 69, 659 (1956); R. J. W. Henry and N. F. Lane, Phys. Rev. 183, 221 (1969); R. W. B. Andill and W. D. Davison, Proc. R. Soc. A 304, 465 (1968); B. D. Buckley and P. G. Burke, J. Phys. B 10, 725 (1977); Y. Itikawa and O. Ashihara, J. Phys. Soc. Jpn. 30, 1461 (1971).
[51]J. C. Slater, *Quantum Theory of Atomic Structure* (McGraw-Hill, New York, 1968), Vol. 2, Chap. 17; M. E. Riley and D. G. Truhlar, J. Chem. Phys. 63, 2182 (1975).
[52]D. G. Truhlar and M. A. Brandt, J. Chem. Phys. 65, 3092 (1976); D. G. Truhlar, R. E. Poling, and M. A. Brandt, *ibid.* 64, 826 (1976); P. Baille and J. W. Dare-

wych, J. Phys. B 10, 615 (1977).
[53]P. G. Burke and N. Chandra, J. Phys. B 5, 1696 (1972).
[54]See Refs. 7, 21, 22, and references therein. Similar types of models are used in Refs. 12, 20, 25, and 29.
[55]A. D. McLean and M. Yoshimine, IBM J. Res. Dev. 12, 206 (1968); and Int. J. Quantum Chem. 81, 313 (1967).
[56]Landolt-Börnstein, *Numerical Data and Functional Relationships in Science and Technology, Group* II, *Atomic and Molecular Physics*, edited by K. H. Hellwege and A. M. Hellwege (Springer-Verlag, Berlin, 1974), Vol. 6.
[57]See H. F. Schaeffer, *The Electronic Structure of Atoms and Molecules* (Addison-Wesley, Reading, Mass., 1972).
[58]R. M. Stevens and W. N. Lipscomb, J. Chem. Phys. 41, 184 (1964).
[59]H. J. Kolker and M. Karplus, J. Chem. Phys. 39, 2011 (1963).
[60]R. G. Newton, *Scattering Theory of Waves and Particles* (McGraw-Hill, New York, 1966).
[61]W. N. Sams and D. J. Kouri, J. Chem. Phys. 51, 4809 (1969); 51, 4815 (1969).
[62]R. A. White and E. F. Hayes, J. Chem. Phys. 57, 2985 (1972).
[63]O. H. Crawford and A. Dalgarno, J. Phys. B 4, 494 (1971).
[64]Cross sections in the complete representation were obtained using the program of M. A. Brandt, D. G. Truhlar, and R. L. Smith [Comput. Phys. Commun. 5, 456 (1973); 7, 177 (1974)].
[65]The actual integration mesh for LiF was as follows: $0.0-3.0a_0$ at $0.01a_0$, $3.0-10.0a_0$ at $0.1a_0$, $10.0-50.0$ at $0.25a_0$, $50.0-100.0a_0$ at $0.5a_0$, and $100.0-R_{max}$ at $1.0a_0$.
[66]The values of l_{max}, λ_{max} (λ_e) needed for the other alkali-metal halides are as follows: LiCl—20, 40(24), NaF—30, 40(24), NaCl—42, 45(24).
[67]L. G. Christophorou, G. S. Hurst, and W. G. Hendrick, J. Chem. Phys. 45, 1081 (1967).
[68]L. G. Christophorou and A. A. Christodoulides, J. Phys. B 2, 71 (1969).
[69]The results of reanalysis of the data of L. G. Christophorou and D. Pittman [J. Phys. B 3, 1252 (1970)] by I. I. Fabrikant [J. Phys. B 10, 1761 (1977)].
[70]K. D. Jordan and W. Luken, J. Chem. Phys. 64, 2760 (1976).
[71]B. I. Schneider, Phys. Rev. A 14, 1923 (1976).
[72]W. J. Stevens (private communication)
[73]M. Krauss and F. H. Mies, Phys. Rev. A 1, 1592 (1970).
[74]See, for example, Refs. 40 and 49.
[75]Resonances have been observed in photodetachment of NaCl, NaBr, and NaI by S. E. Novick, P. L. Jones, T. J. Mulloney, and W. C. Lineberger (private communication), estimated to lie ~1.5 eV above the ground state.
[76]R. C. Stern and W. Becker, in *Abstracts of Papers, Ninth International Conference on the Physics of Electronic and Atomic Collisions*, edited by J. S. Risley and R. Geballe (University of Washington, Seattle, 1975), p. 275.
[77]I. Shimamura (private communication).